

Supporting information

One-Atom-Substitution Enables Direct and Continuous Monitoring of Histone Deacetylase Activity

*Matthes Zessin[§], Zsófia Kutil[‡], Marat Meleshin[†], Zora Nováková[‡], Ehab Ghazy[§], Diana Kalbas[†],
Martin Marek[§], Christophe Romier[§], Wolfgang Sippl[§], Cyril Bařínka[‡], Mike Schutkowski^{†*}*

[§] Department of Medical Chemistry, Institute of Pharmacy, Martin-Luther-University Halle-
Wittenberg, 06120 Halle/Saale, Germany

[†] Department of Enzymology, Institute of Biochemistry and Biotechnology, Charles-Tanford-
Protein Center, Martin-Luther-University Halle-Wittenberg, 06120 Halle/Saale, Germany

[‡] Institute of Biotechnology of the Czech Academy of Sciences, BIOCEV, Prumyslova 595, 252
50 Vestec, Czech Republic.

[§] Departement de Biologie Structurale Integrative, Institut de Genetique et Biologie Molculaire
et Cellulaire (IGBMC), Universite de Strasbourg (UDS), CNRS, INSERM, 1 rue Laurent Fries,
B.P. 10142, 67404 Illkirch Cedex IGBMC, France

Table of content

Table S1. The source of genes encoding individual human HDACs used in this study.....	3
Table S2. Kinetic parameters of peptide 3 and peptide 2	10
Table S3. Values for the calculation of the Z' factor and signal noise ratio.	23
Figure S1. Coomassie-stained SDS-PAGE of purified HDAC4, 5, 6, 7, 8 and 10.....	4
Figure S2. Schematic representation of the expression plasmid for full-length human HDAC6..	5
Figure S3. UV-Vis spectra of 2 , thioacetate and difference spectra.	6
Figure S4. Absorbance (left) and fluorescence (right) spectra of peptide 1 , 2 , 3 and 5	6
Figure S5. Absorbance spectra of peptide 12 in comparison to peptide 5	7
Figure S6. Absorbance (left) and fluorescence (right) spectra of peptide 13	7
Figure S7. Absorbance spectra of peptide 10 , 9 and 8 (left).	8
Figure S8. Detection of free thiomyristic acid with Ellmans's reagent.	9
Figure S9. v/[S]-plot of HDAC 8 and 6 with peptide 2 and 3	11
Figure S10. v/[S]-plot of different HDAC isoforms with peptide 5	12
Figure S11. v/[S]-plot of different HDAC isoforms with peptide 4	13
Figure S12. Steady-state kinetics of HDAC6 on Abz-SRGG[K-Sformyl/Spropionyl]FFRR peptides.	14
Figure S13. Dose-response analysis for HDAC4.....	15
Figure S14. Dose-response analysis for HDAC5.....	16
Figure S15. Dose-response analysis for the inhibitors LMK-235 and HDAC6.	17
Figure S16. Dose-response analysis for HDAC8 part 1.	18
Figure S17. Dose-response analysis for HDAC8 part 2.	19
Figure S18. Inhibition of different HDAC isoforms through thioacetate and Abz-SRGGK(Me, Ac)FFRR-NH ₂	20
Figure S19. Dose-response analysis for Abz-SRGGK(My, Me)FFRR-NH ₂ and HDAC11.	21
Figure S20. v/[S]-plot of HDAC11 with peptide 9 and 10	21
Figure S21. Fluorescence intensity/time-plot for determination of Z' factor.	22
Figure S22. UPLC profile of the deacylation of peptide 13 by HDAC8.	24
Figure S23. v/[S]-plot of smHDAC isoforms with peptide 4 and 5	25
Figure S24. UPLC-MS profile of peptide 2	26
Figure S25. UPLC-MS profile of peptide 4	27
Figure S26. UPLC-MS profile of peptide 6	28
Figure S27. UPLC-MS profile of peptide 11	29
Figure S28. UPLC-MS profile of peptide 12	30
Figure S29. UPLC-MS profile of peptide 13	31
Figure S30. UPLC-MS profile of peptide 8	32
Figure S31. UPLC-MS profile of peptide 10	33
Figure S32. UPLC-MS profile of peptide 9	34

Table S1. The source of genes encoding individual human HDACs used in this study, their GenBank ID (<http://www.ncbi.nlm.nih.gov>) and list of primers used for their cloning

Gene	Source	Gene ID	bank	Amino acids	Primer sequence, 5'–3'
<i>HDAC1</i>	Addgene ¹	NM_004964		1-482	F: GAGAACCTGTACTTCCAGGGCGGAGGCaccATGGCGCAGACGCAGGGCACCCGGAGG R: GGGGACCACTTTGTACAAGAAAGCTGGGTTATTAGGCCAACTTGACCTCCTCCTTGACC
<i>HDAC4</i>	Addgene ²	NM_006037.2		1-1084	F: GAGAACCTGTACTTCCAGGGCGGAGGCACCATGAGCTCCCAAAGCCATCCAGATG R: GGGGACCACTTTGTACAAGAAAGCTGGGTTATTACAGGGGCGGCTCCTCTTCCATGGG
<i>HDAC5*</i>	Addgene ²	NM_005474		679-1095	F: GAGAACCTGTACTTCCAGGGCGGAGGCACCATGAACTCTCCCAACGAGTCGGATGGG R: GGGGACCACTTTGTACAAGAAAGCTGGGTTATTACAGGGCAGGCTCCTGCTCCATGGG
<i>HDAC6</i>	Open Biosystems	NM_006044.3		1-1215	F: GAGAACCTGTACTTCCAGTCTATGACCTCAACCGGCCAGGATTCCAC R: GAGGATATGCCCCACCCACACTAATAACCCAGCTTTCTTGTACAAAGTGGTCCCC
<i>HDAC7</i>	Addgene ²	NM_016596		1-915	F: GAGAACCTGTACTTCCAGGGCGGAGGCACCATGGACCTGCGGGTGGGCCAGCGG R: GGGGACCACTTTGTACAAGAAAGCTGGGTTATTAGAGATTTCATAGGTTCTTCCTCCTC
<i>HDAC8</i>	Prof. M. Schutkowski, PhD, Martin Luther University Halle	NM_018486.3		1-377	F: TCGGAGAACCTGTACTTCCAGTCTACCATGGAGGAGCCGGAGGAACCGGCGG R: GGGGACCACTTTGTACAAGAAAGCTGGGTTATTAAGACCACATGCTTCAGATTCCCTTTG
<i>HDAC9</i>	D. Mauceri, PhD, University of Heidelberg	NM_178425.3		1-1069	F: GAGAACCTGTACTTCCAGGGCGGAGGCACCATGCACAGTATGATCAGCTCAGTG R: GGGGACCACTTTGTACAAGAAAGCTGGGTTATTACAAGGCTGGCTCCTCTTCCATAGG R: GGGACCACTTTGTACAAGAAAGCTGGGAGAGCCAGAACCCTGGAAGTACAGGTTCTCAG
<i>HDAC11</i>	Prof. E. Seto (The George Washington University)	NP_079103.2		1-346	F: GAGAACCTGTACTTCCAGGGCGGAGGCACCATGCTACACACAACCCAGCTGTAC R: AGACTGGAAGTACAGGTTCTCAGAACCGGGCACTGCAGGGGGAAGCAG
-					F2-general: GGGGACAAGTTTGTACAAAAAAGCAGGCTCGGAGAACCTGTACTTCCAG

*Due to the low expression level of full length HDAC5, only the catalytic domain spanning the residues H679 - G1095 was cloned into the expression vector

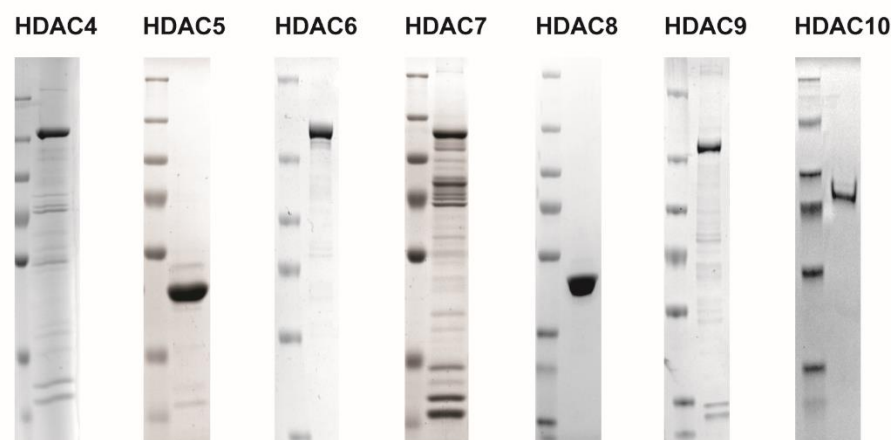


Figure S1. Coomassie-stained SDS-PAGE of purified HDAC4, 5, 6, 7, 8 and 10.

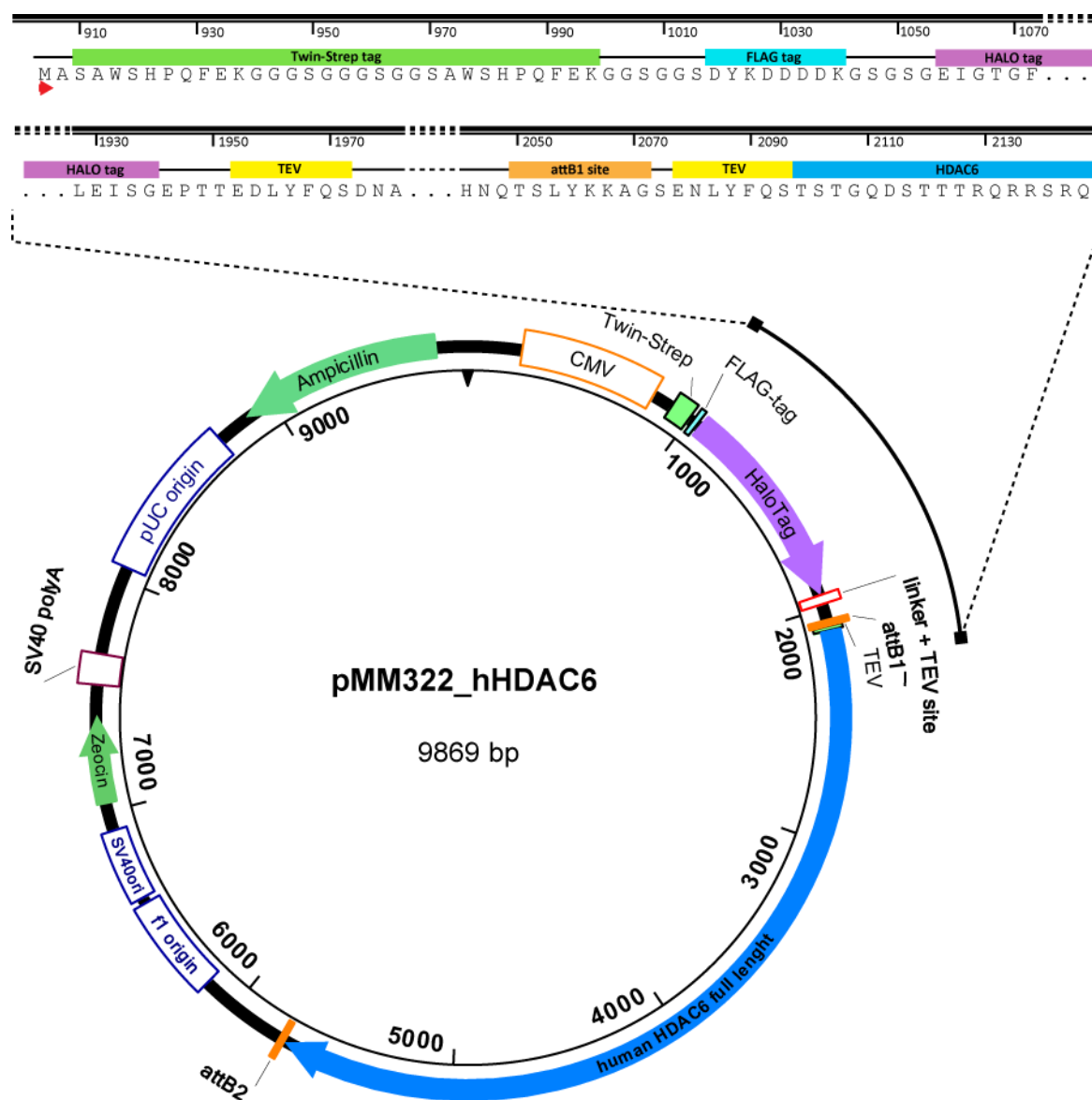


Figure S2. Schematic representation of the expression plasmid for full-length human HDAC6.

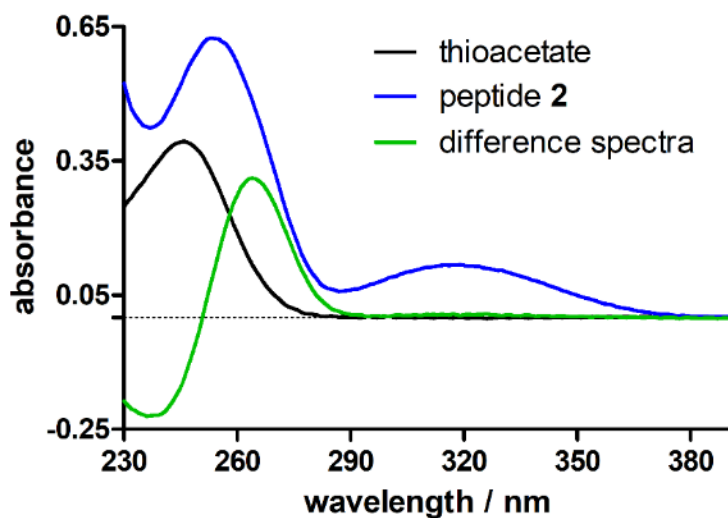


Figure S3. UV-Vis spectra of **2**, thioacetate and difference spectra which is calculated from the difference of absorbance of **2** and absorbance of thioacetate. The concentration of the compounds was 50 μ M.

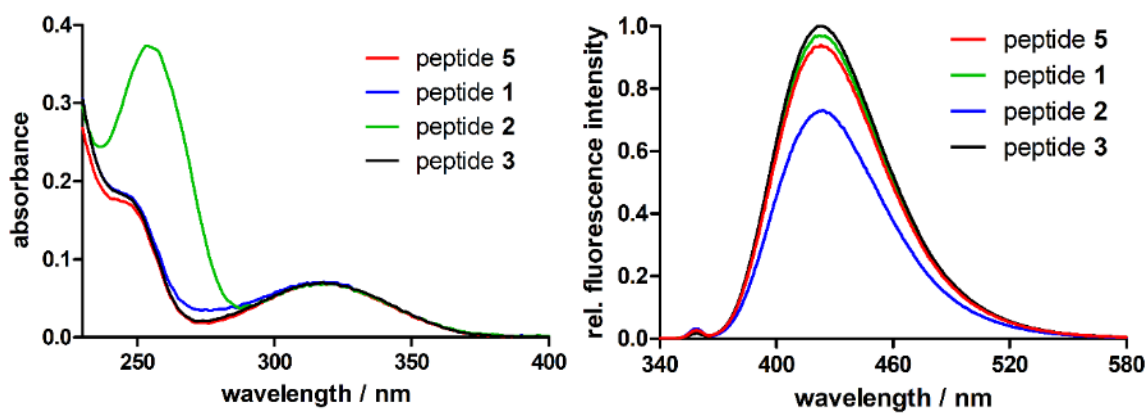


Figure S4. Absorbance (left) and fluorescence (right) spectra of peptide **1**, **2**, **3** and **5**. The excitation wavelength of the fluorescence spectra was 320 nm. The measurements take place at 25 $^{\circ}$ C.

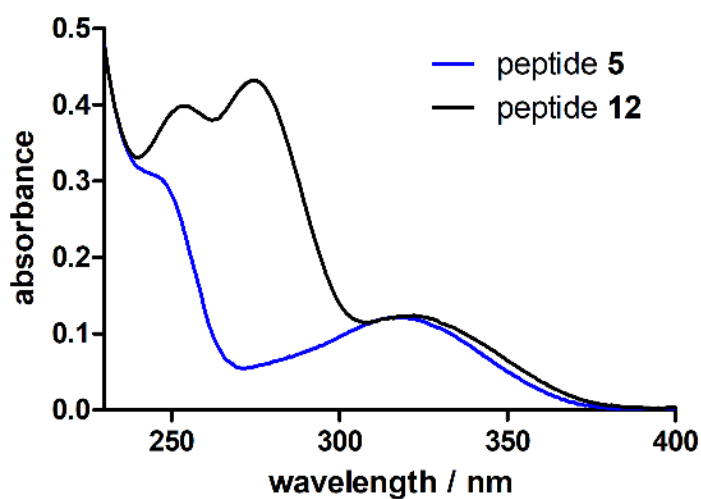


Figure S5. Absorbance spectra of peptide 12 in comparison to peptide 5.

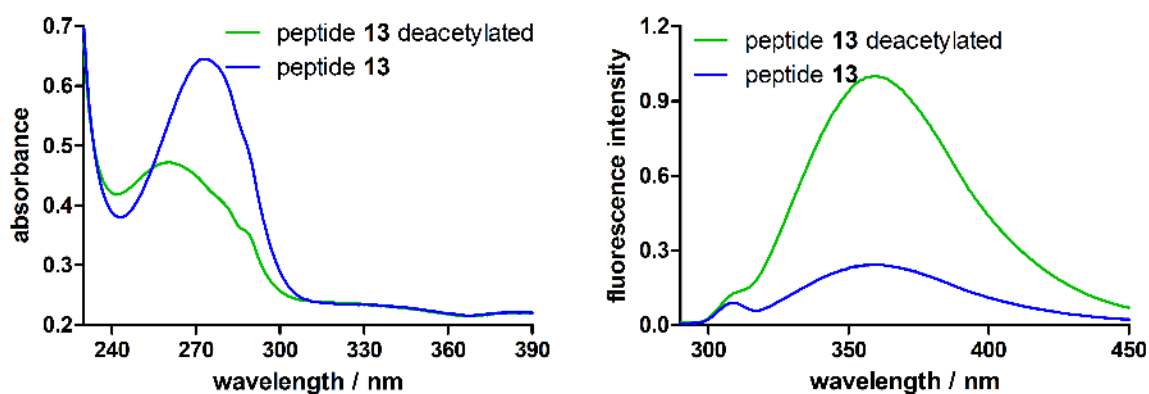


Figure S6. Absorbance (left) and fluorescence (right) spectra of peptide 13 and peptide 13 in deacetylated form. The excitation wavelength of the fluorescence spectra was 280 nm. The measurements take place at 25 °C.

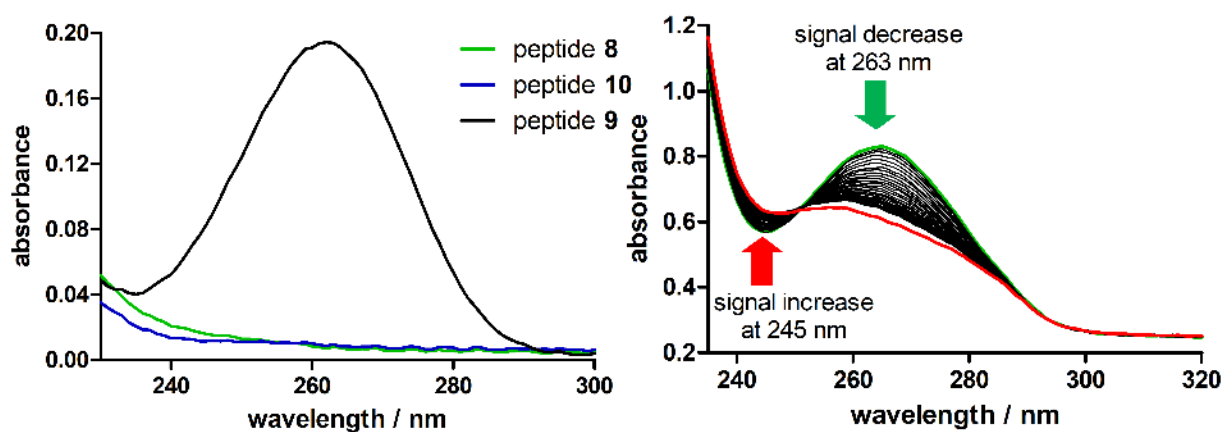


Figure S7. Absorbance spectra of peptide 10, 9 and 8 (left). Spectra kinetic of HDAC11 and peptide 9. Peptide concentration was 50 μM and HDAC11 concentration 0,1 μM . The reaction take place at 37 $^{\circ}\text{C}$ in a 100 μl cuvette. The green line shows the first spectra after addition of HDAC11. Every black line shows a spectrum after 80 s. The red line shows the last recorded spectrum after 66 min.

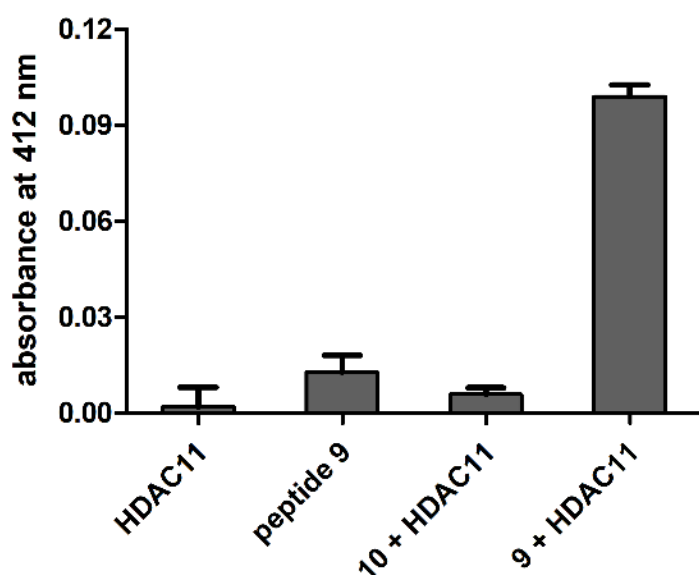


Figure S8. Detection of free thiomyristic acid. The reaction mixture was incubated for at least 1 h at 37 °C. The mixture contains 0,1 μ M HDAC11, 50 μ M of peptide **9** or **10**) in buffer (20 mM phosphoric acid pH 7.4 adjusted with NaOH and 0,2 mg/ml BSA). 50 μ l of the reaction mixture was mixed with 100 μ l buffer (20 mM phosphoric acid pH 7.4 adjusted with NaOH) and 7.5 μ l developing reagent (20 mM 5,5'-dithiobis-(2-nitrobenzoic acid) and 100 mM EDTA). The mixture was incubated at 37°C for 30 min and the readout was done with UV/vis photometer at a wavelength at 412 nm. The samples were blanked against buffer with the developing reagent in the same mixing ratio as above.

Table S2. Kinetic parameters of peptide **3** and peptide **2**.

	peptide 3			peptide 2		
HDAC	$K_M / \mu\text{M}$	$k_{\text{cat}} / \text{s}^{-1}$	$k_{\text{cat}} / K_M / \text{M}^{-1} \cdot \text{s}^{-1}$	$K_M / \mu\text{M}$	$k_{\text{cat}} / \text{s}^{-1}$	$k_{\text{cat}} / K_M / \text{M}^{-1} \cdot \text{s}^{-1}$
1	8.5 % ^[b]			0 % ^[a]		
4	0 % ^[a]			0 % ^[a]		
5	0 % ^[a]			3.8 % ^[a]		
6	12 ³	2 ³	190,000 ³	67 ± 9	0.37 ± 0.02	5500
7	0 % ^[a]			0 % ^[a]		
8	>400	>0.8	n.d.	710 ± 10	13 ± 1	18 000
9	0 % ^[a]			0 % ^[a]		
11	0 % ^[a]			0 % ^[a]		

[a] values show substrate consumption after 1 h incubation of 100 μM of peptide with 0.1 μM corresponding HDAC isoform at 25 °C. [b] no cleavage after 1 h but after 24 h

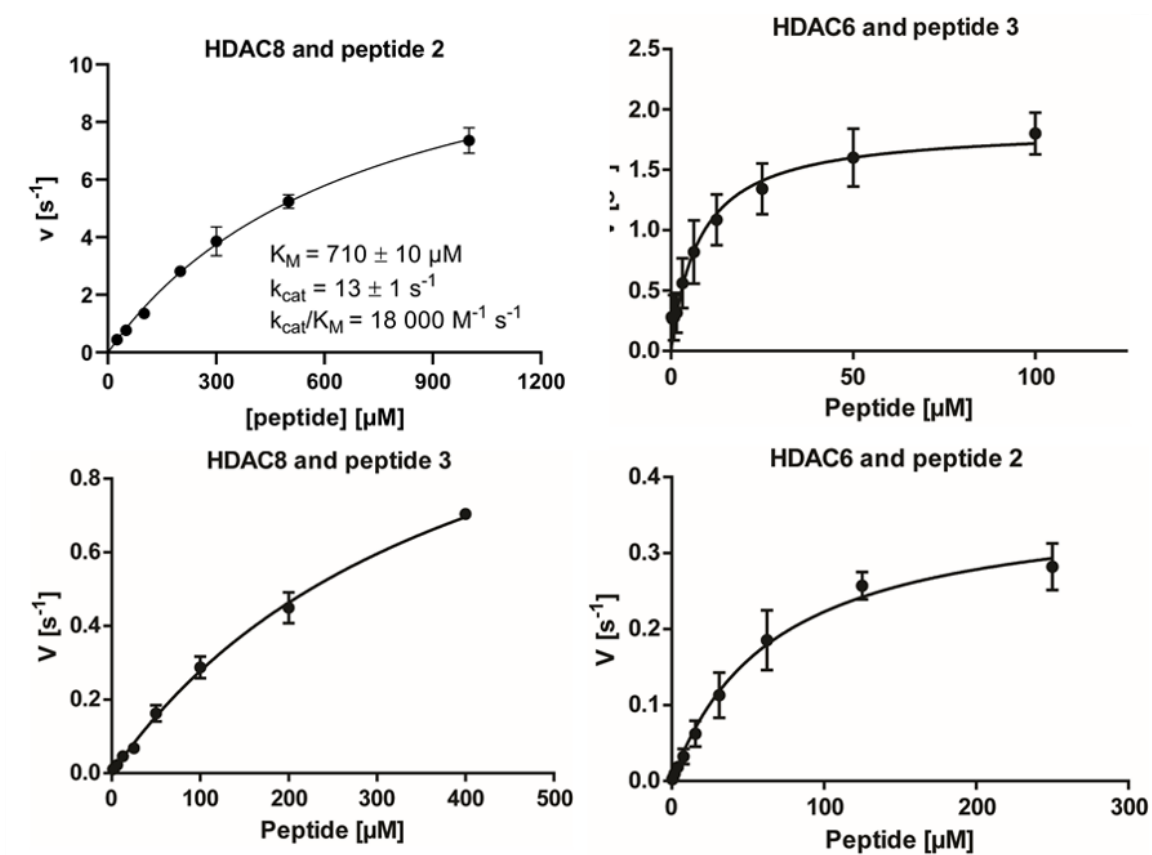


Figure S9. $v/[S]$ -plot of HDAC 8 and 6 with peptide 2 and 3.

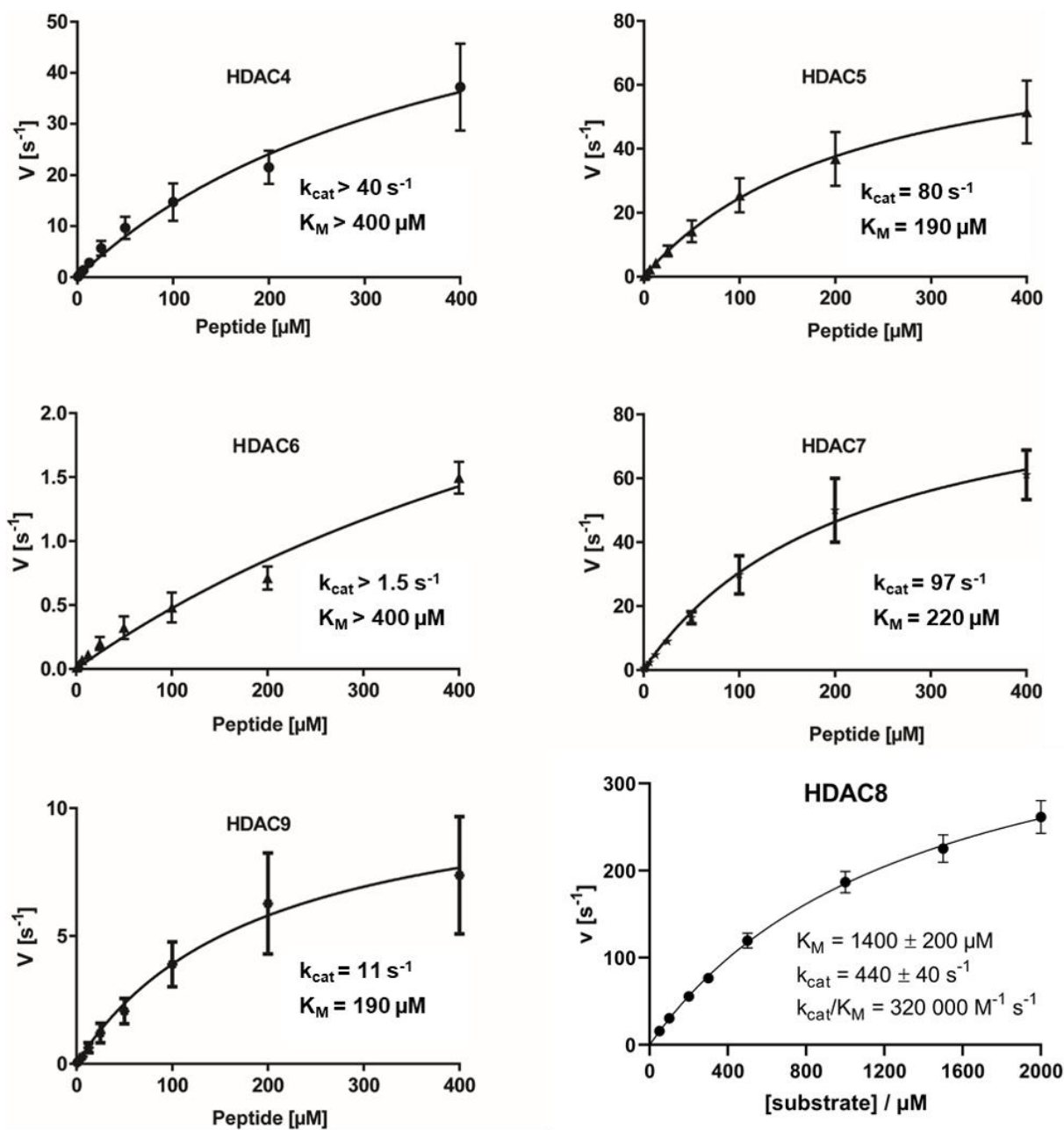


Figure S10. $v/[S]$ -plot of different HDAC isoforms with peptide 5.

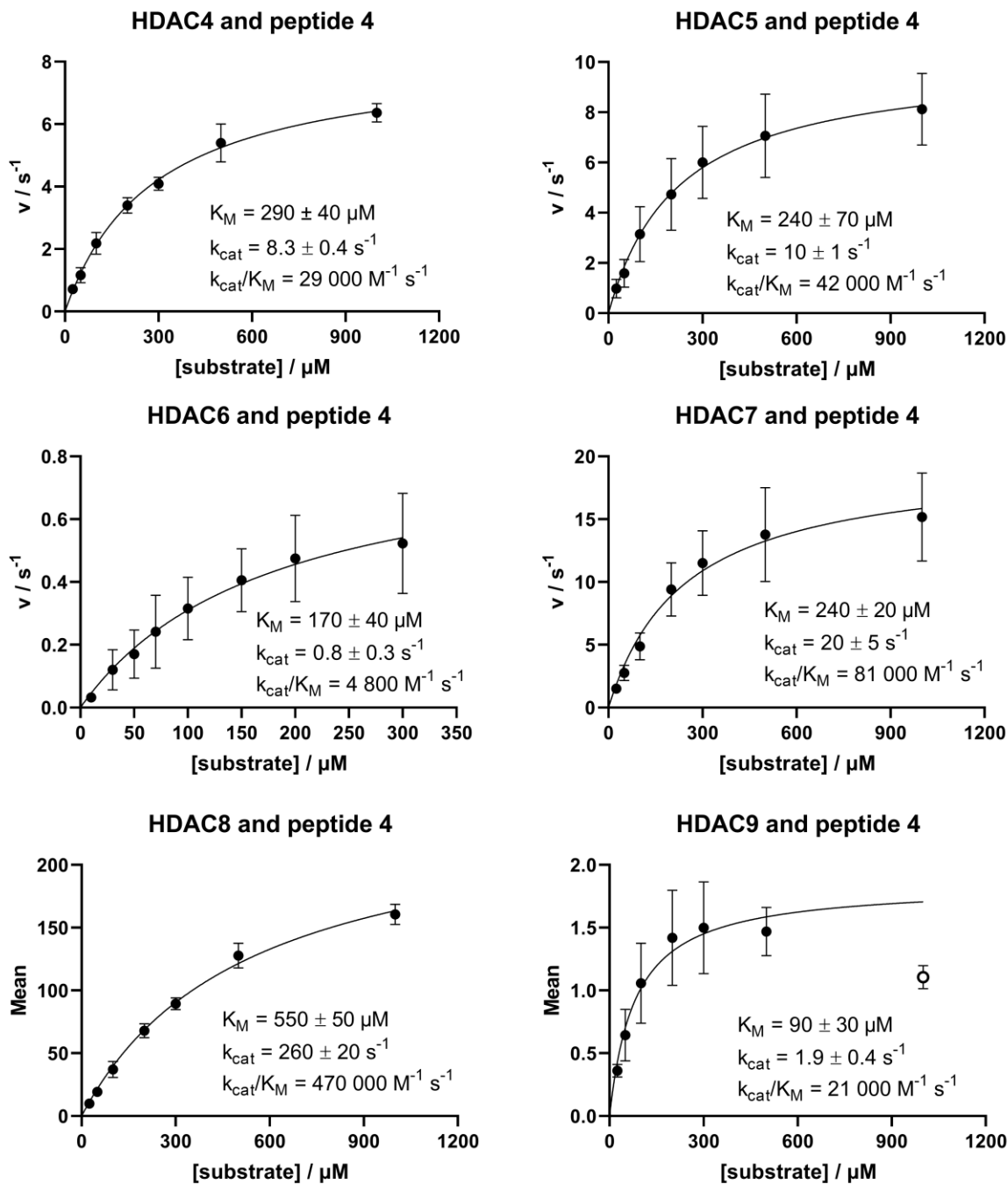


Figure S11. $v/[S]$ -plot of different HDAC isoforms with peptide 4.

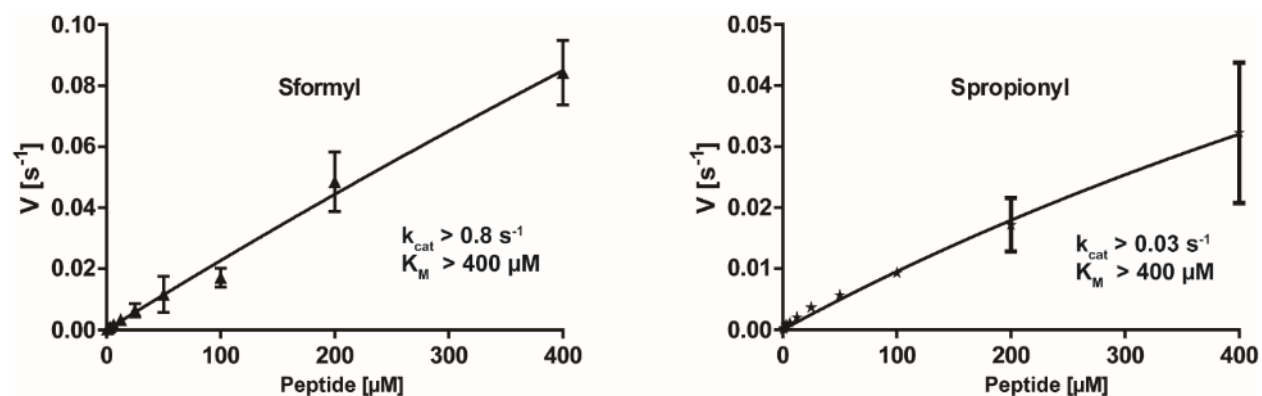


Figure S12. Steady-state kinetics of HDAC6 on Abz-SRGG[K-Sformyl/Spropionyl]FFRR peptides. Optimized concentrations of HDAC6 were mixed with peptide Abz-Ser-Arg-Gly-Gly-Lys-Phe-Phe-Arg-Arg with central Lys modified by Sformyl or Spropionyl in the concentration range 0 – 400 μM and the deacylation reactions proceeded for 30 mins at 37°C. The amount of deacylated substrate was quantified using HPLC.

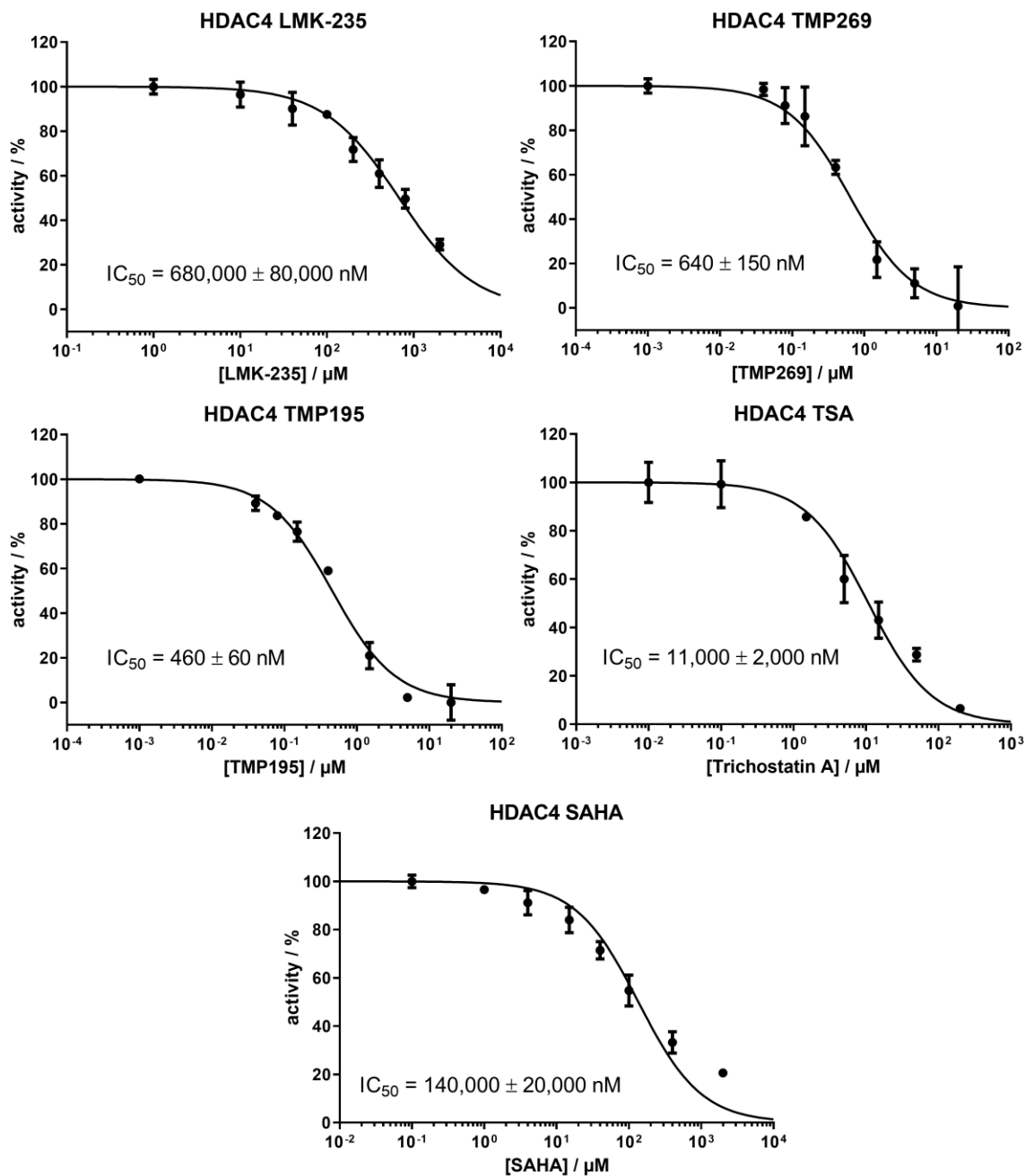


Figure S13. Dose-response analysis for the inhibitors TMP195, TMP269, LMK-235, SAHA and TSA and HDAC4.

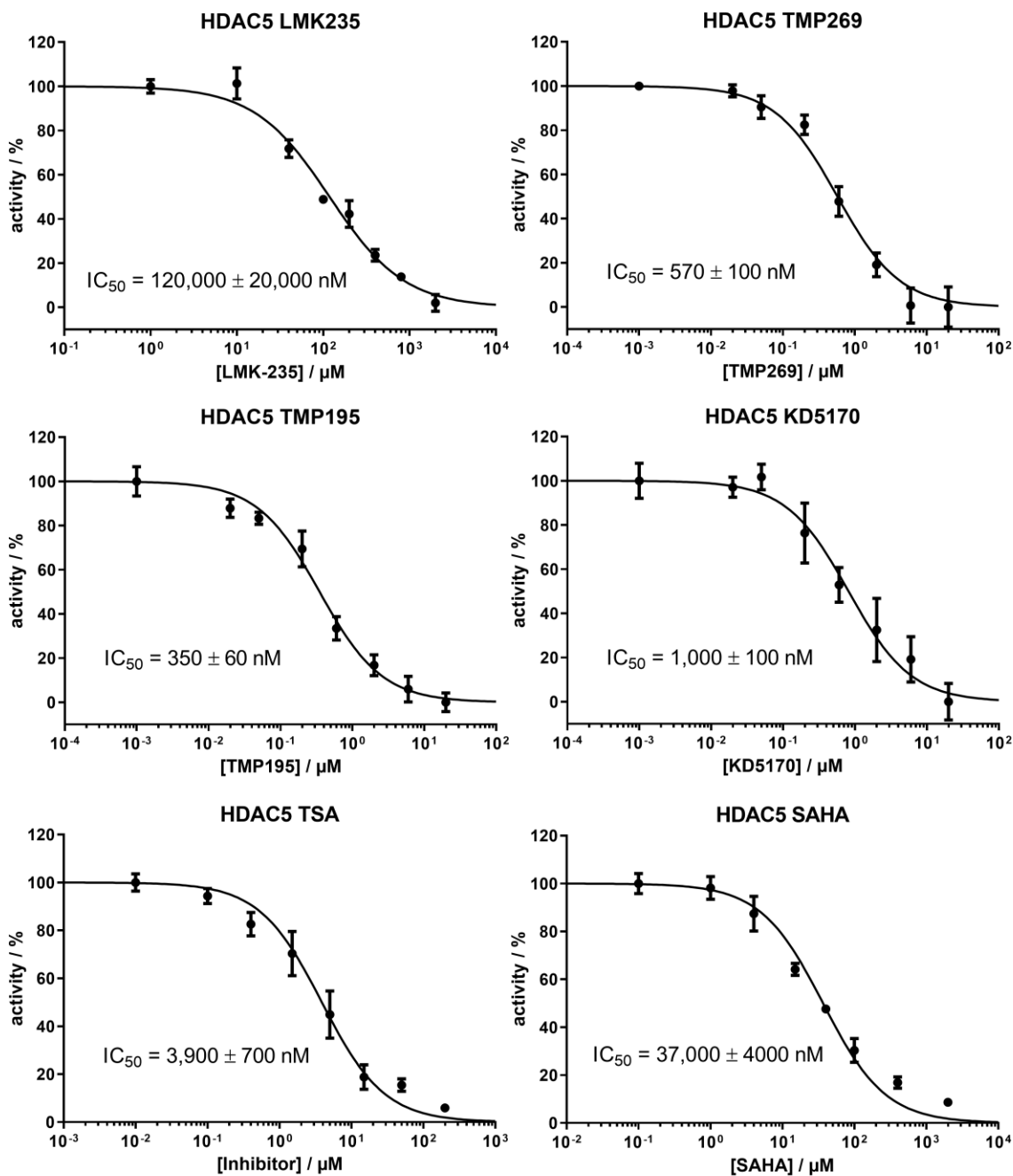


Figure S14. Dose-response analysis for the inhibitors TMP195, TMP269, KD5170, TSA, SAHA and LMK-235 and HDAC5.

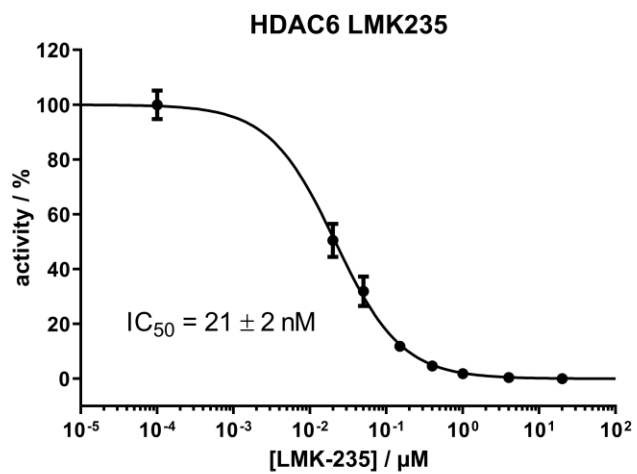


Figure S15. Dose-response analysis for the inhibitors LMK-235 and HDAC6.

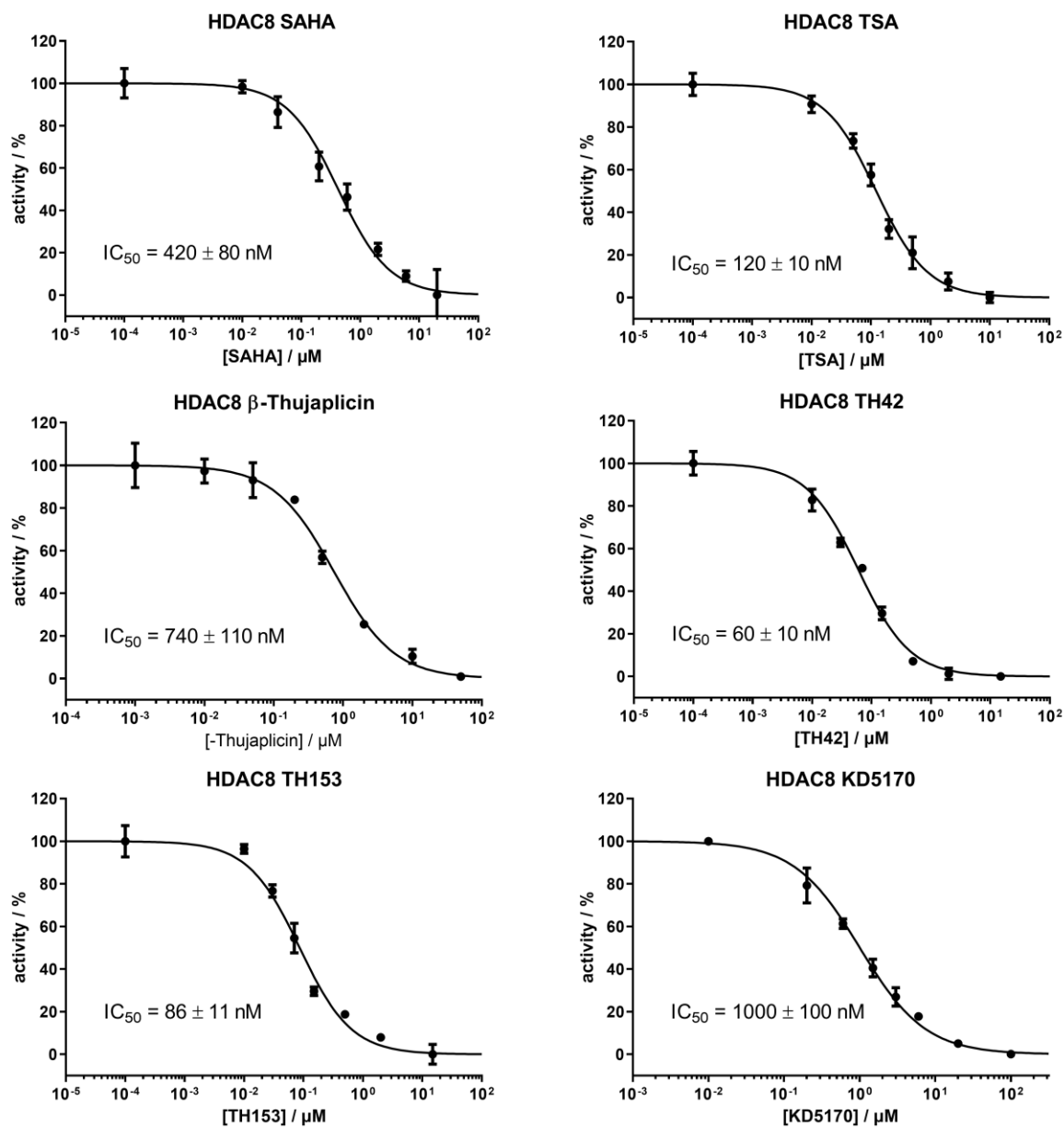


Figure S16. Dose-response analysis for the inhibitors SAHA, Trichostatin A (TSA), β -Thujaplicin, TH42, TH153 and KD5170 and HDAC8.

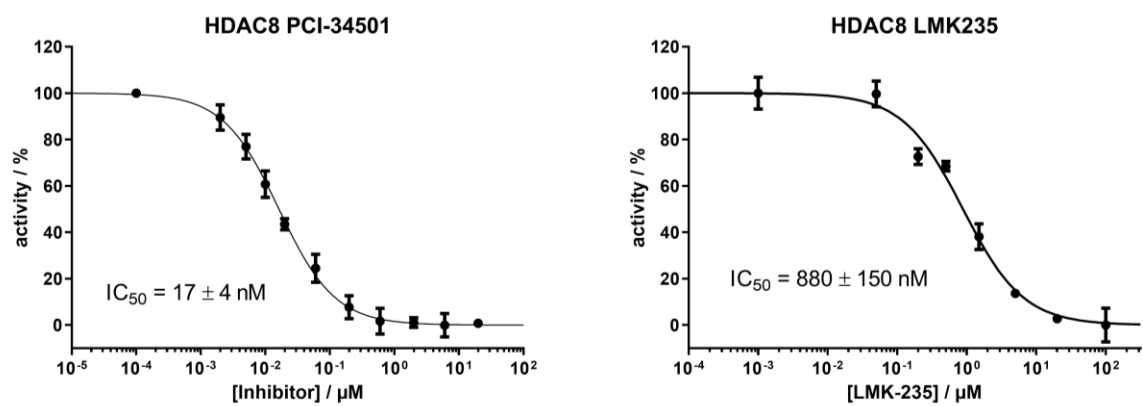


Figure S17. Dose-response analysis for the inhibitors PCI-34501 and LMK-235 and HDAC8.

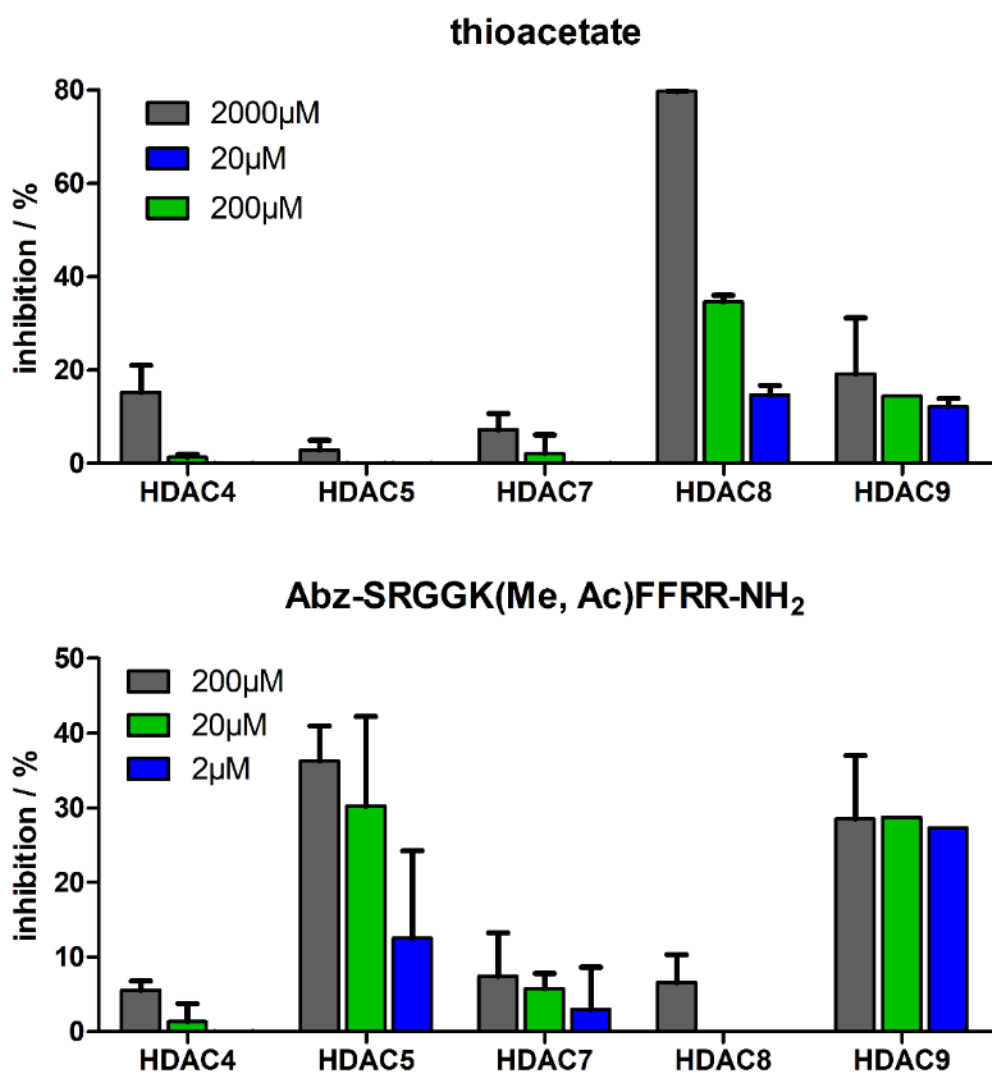


Figure S18. Inhibition of different HDAC isoforms through thioacetate and Abz-SRGGK(Me, Ac)FFRR-NH₂. The substrate was peptide **3** and the substrate consumption was determined by HPLC at a wavelength of 320 nm. Inhibition was calculated from a positive control without inhibitor.

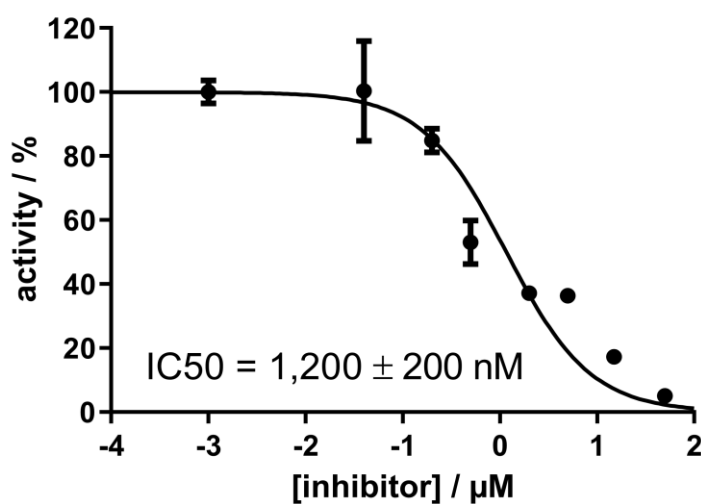


Figure S19. Dose-response analysis for Abz-SRGGK(My, Me)FFRR-NH₂ and HDAC11. The substrate was peptide **5** with a concentration of 50 μM and a HDAC11 concentration of 50 nM. The reaction take place at 37 °C. Product formation was analyzed by HPLC.

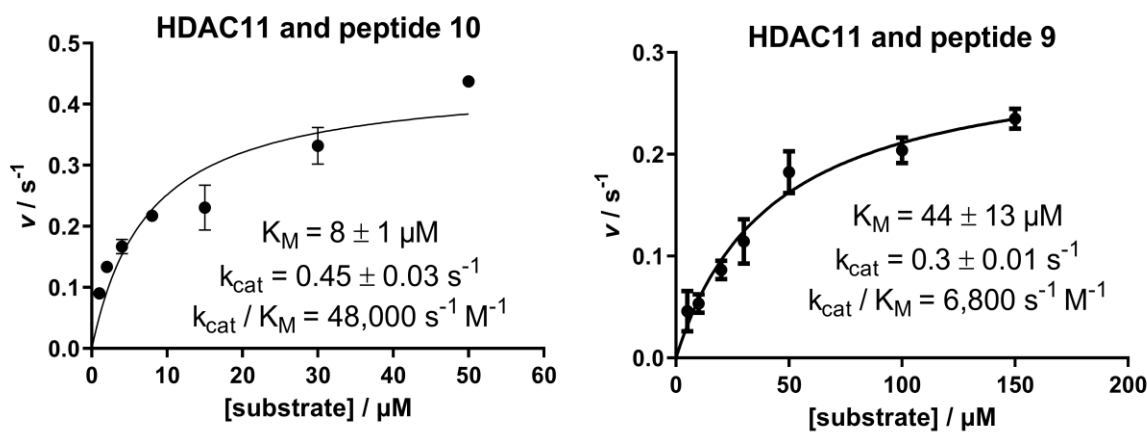


Figure S20. $v/[S]$ -plot of HDAC11 with peptide **9** and **10**. Peptide **9** was measured with UV/Vis-photometer and peptide **10** with HPLC.

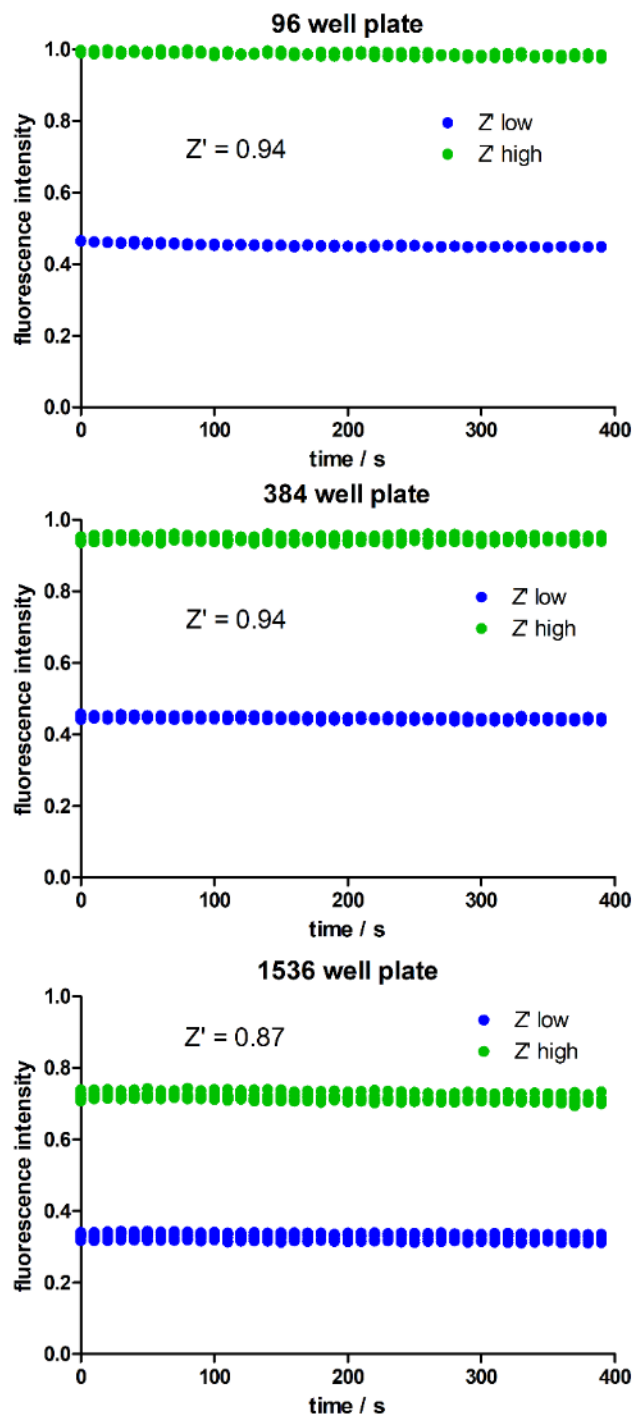
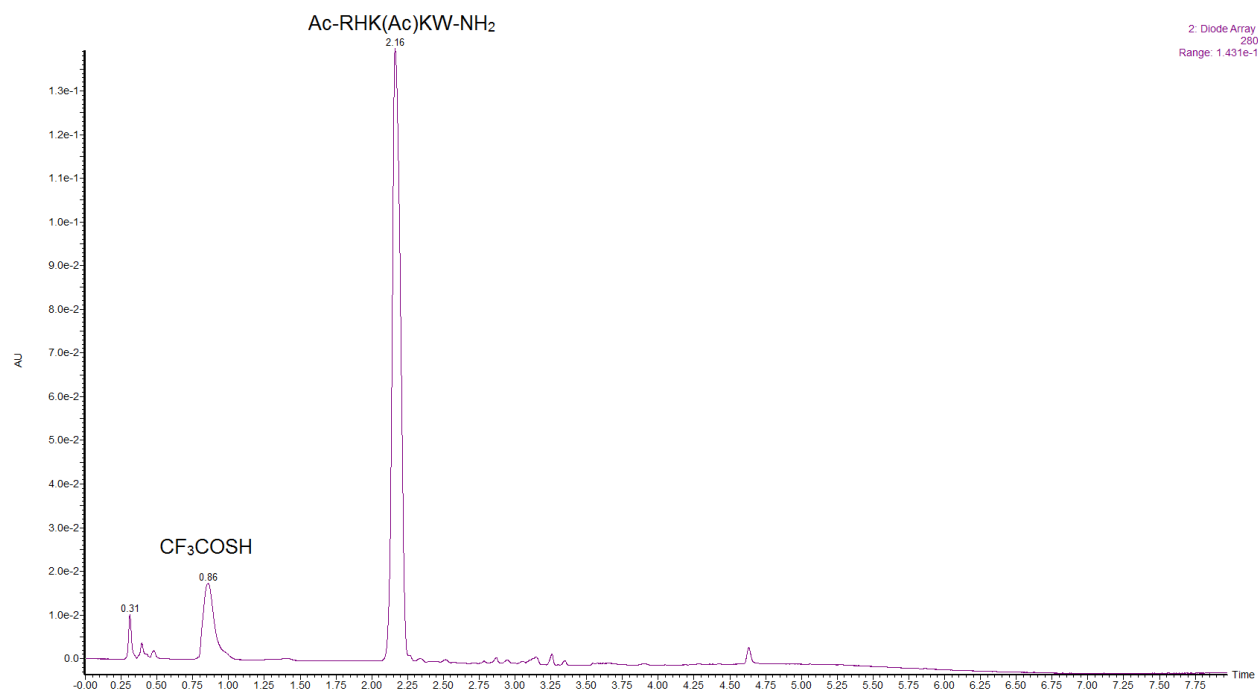
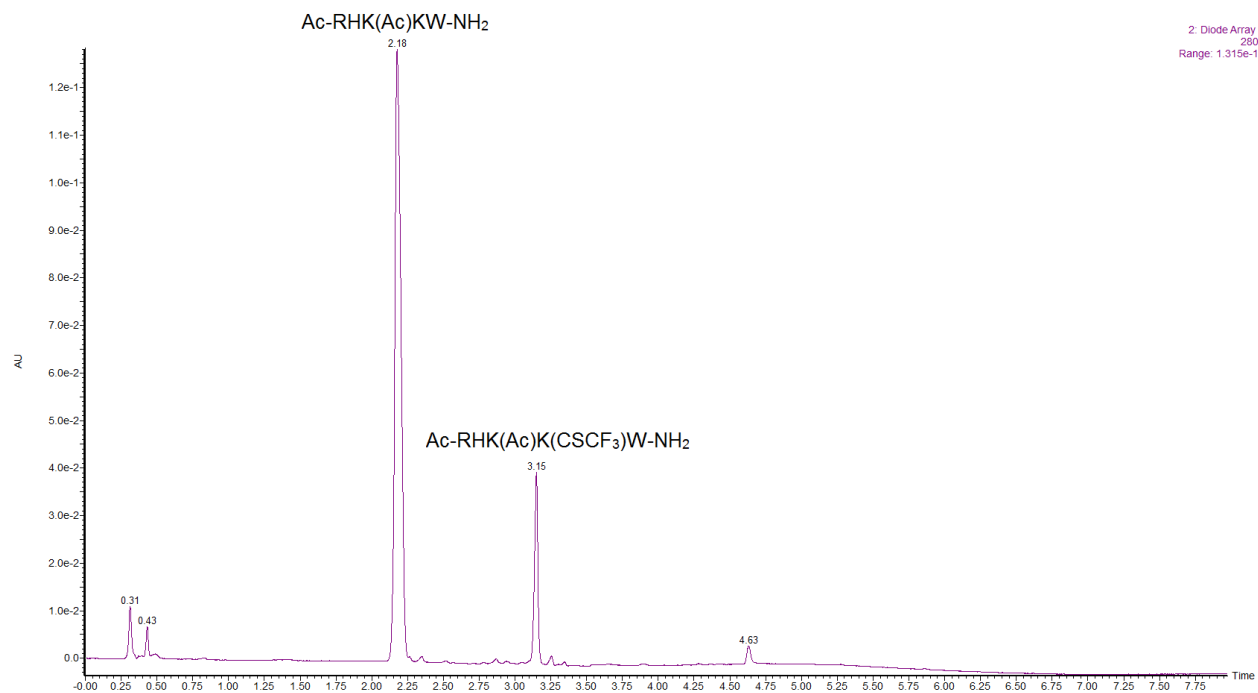
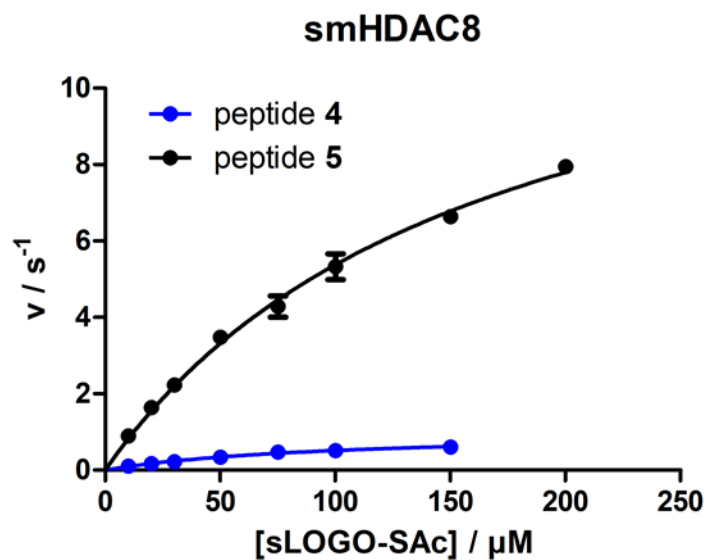


Figure S21. Fluorescence intensity/time-plot for determination of Z' factor. Z' high means full cleaved peptide 4 and Z' low shows peptide 4 without HDAC.

Table S3. Values for the calculation of the Z' factor and signal noise ratio.

	96 well	384 well	1536 well
Mean _{100%}	944787.2	986944.6	716144.4
Mean _{0%}	445505.9	452471.5	330172.4
SD _{100%}	6335.2	6008.9	9233.9
SD _{0%}	4408.1	4607.1	7664.6





peptide	K_M (μM)	k_{cat} (s^{-1})	k_{cat}/K_M ($\text{s}^{-1} \text{M}^{-1}$)
4	100 ± 20	1.0 ± 0.2	10,000
5	160 ± 10	14 ± 1	87,000

Figure S22. $v/[S]$ -plot of smHDAC8 with peptide **4** and **5**. Peptide **5** was measured with HPLC and **4** with UV/Vis-photometer

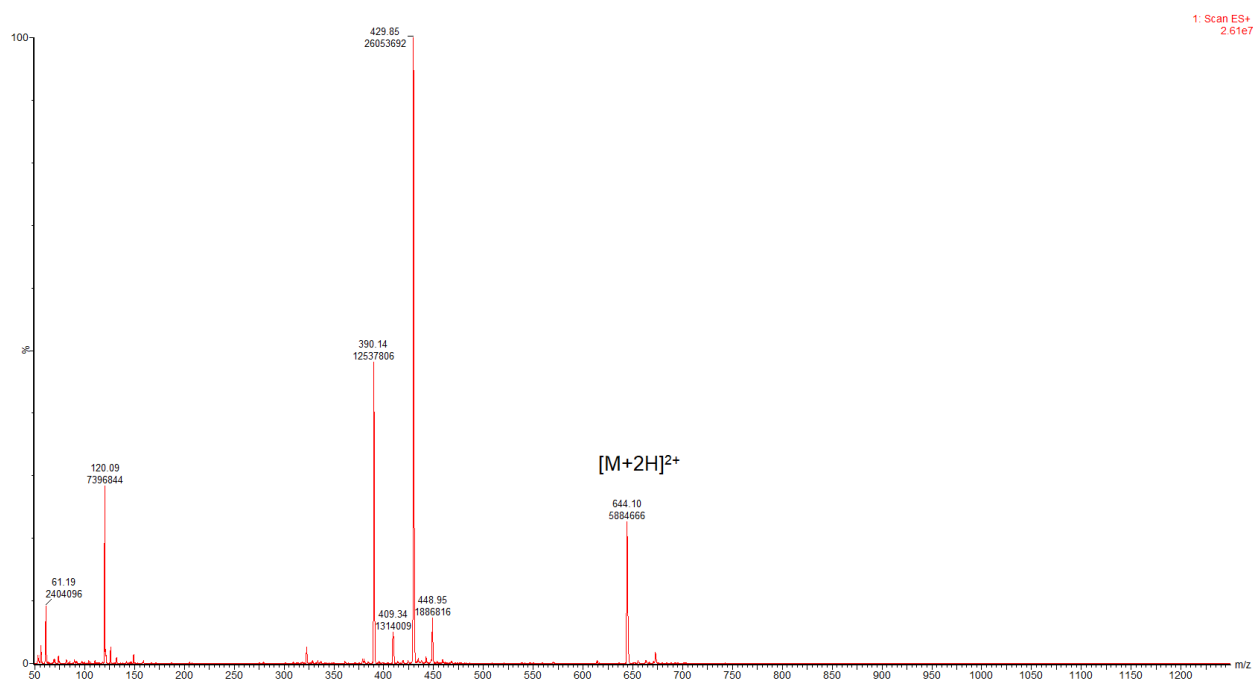
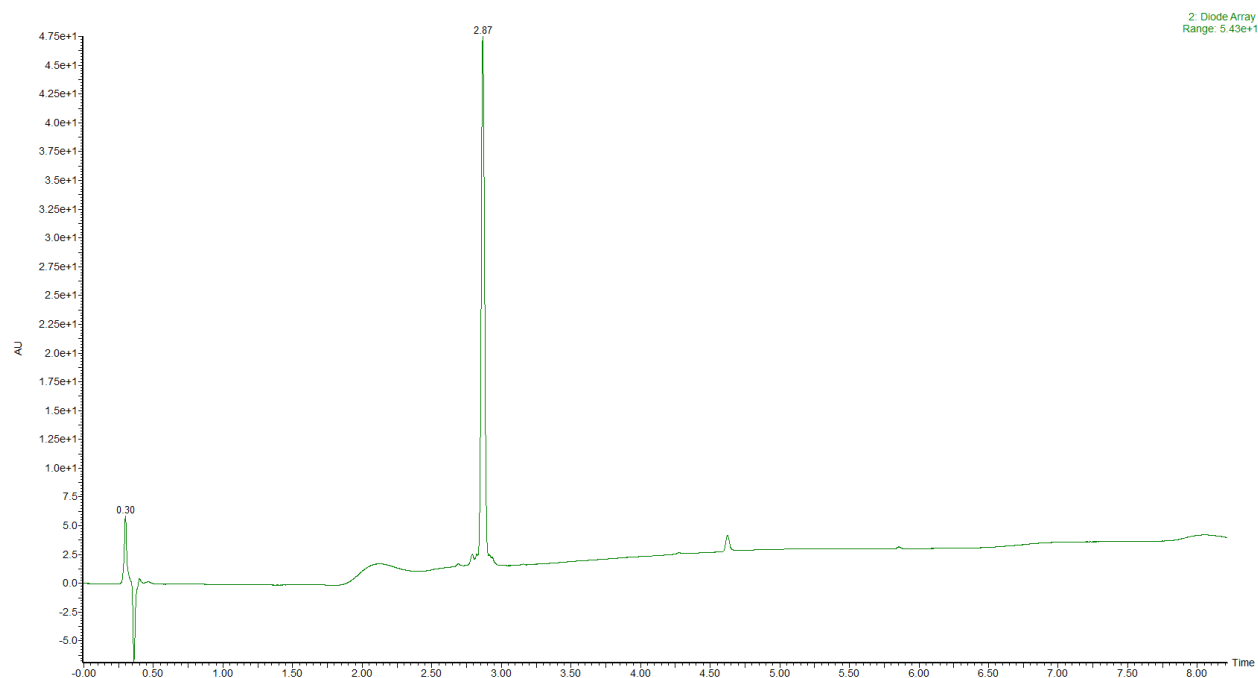


Figure S23. UPLC-MS profile of peptide 2.

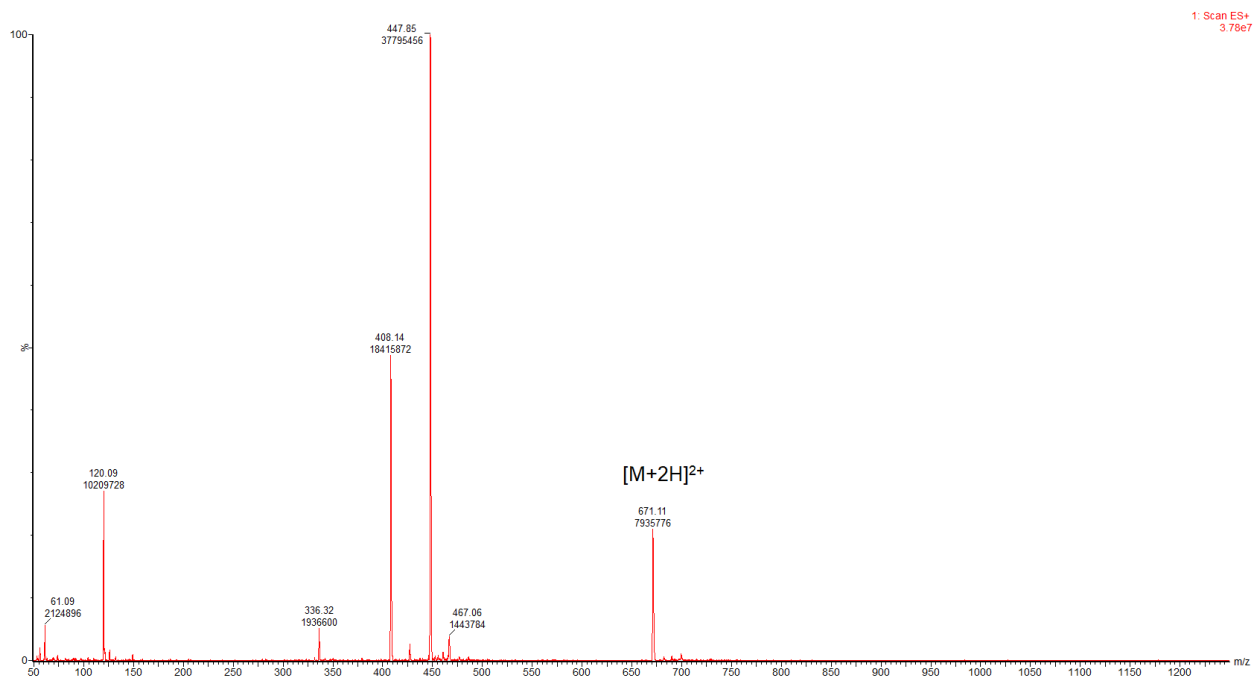
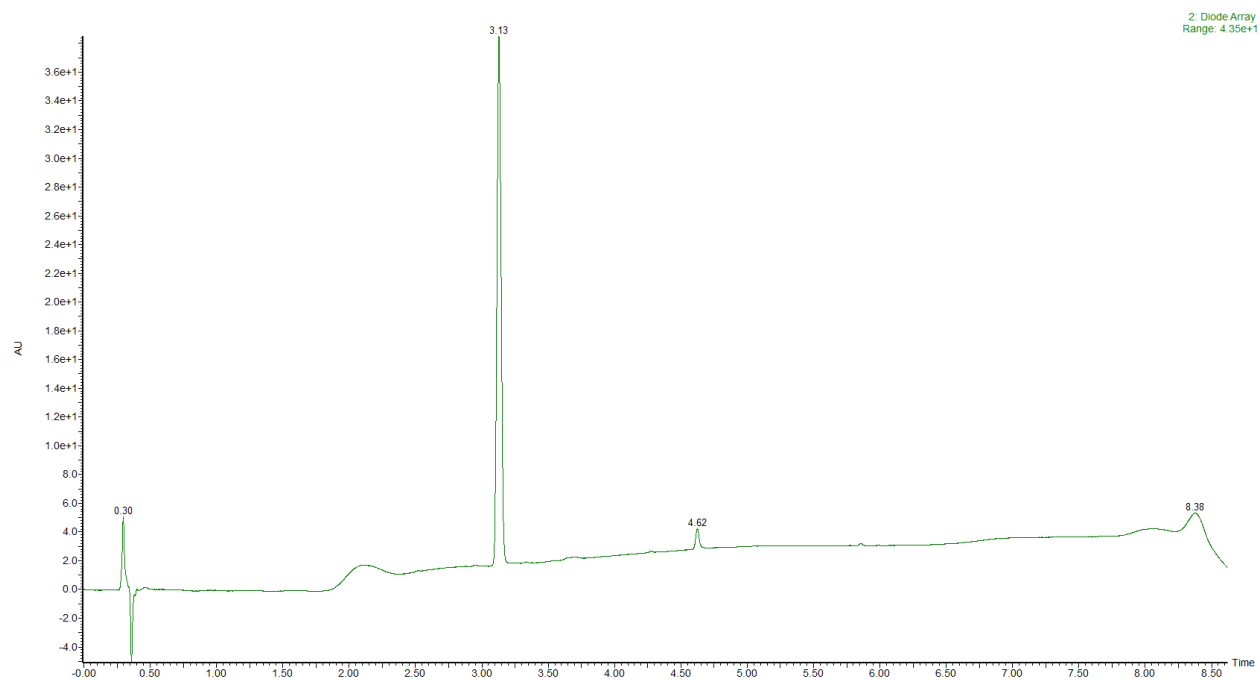


Figure S24. UPLC-MS profile of peptide 4.

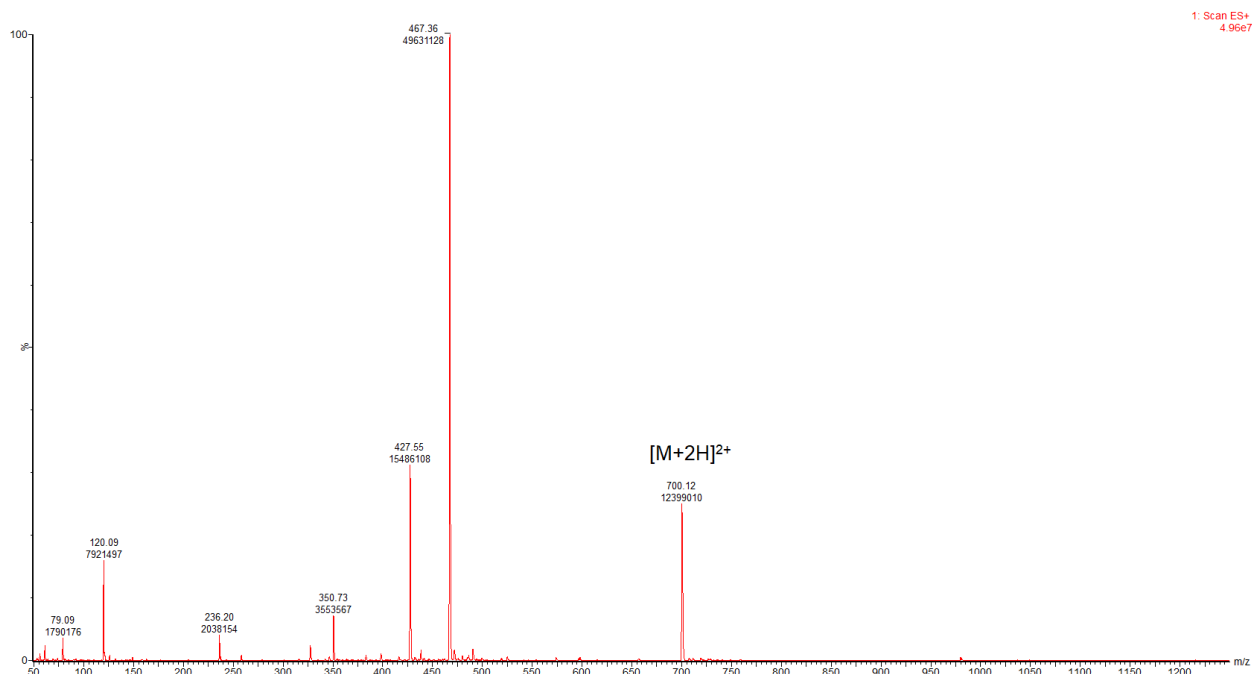
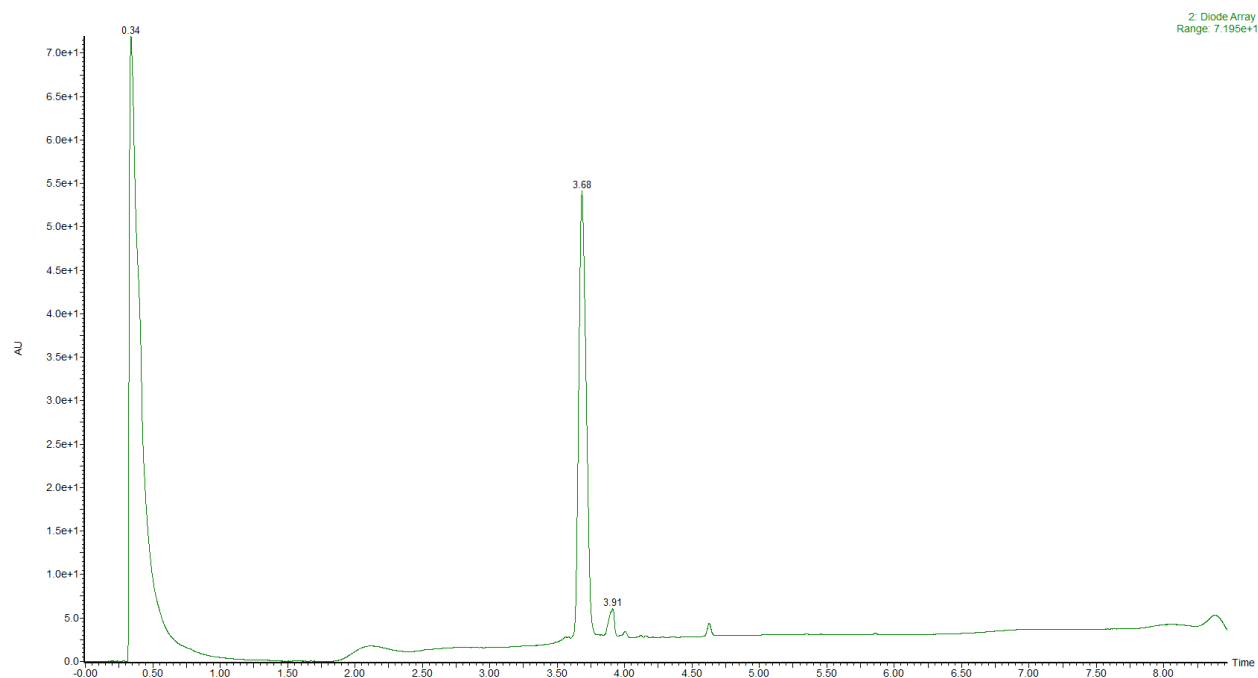


Figure S25. UPLC-MS profile of peptide 6.

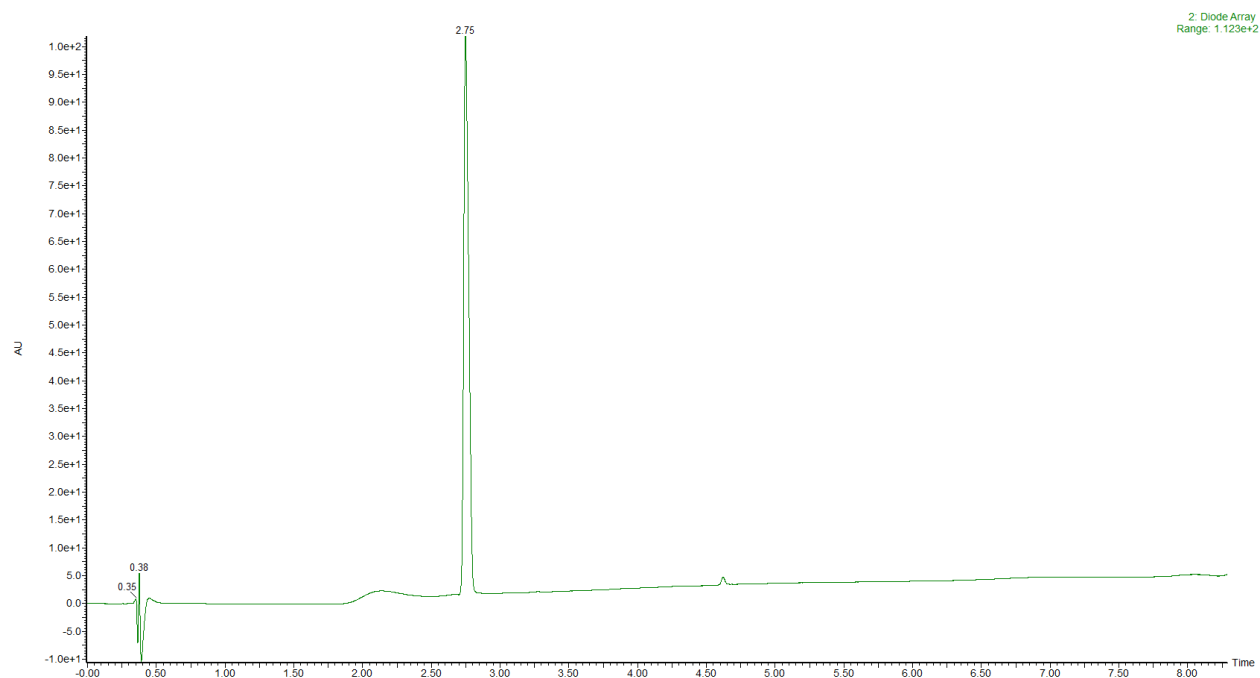


Figure S26. UPLC-MS profile of peptide **11**.

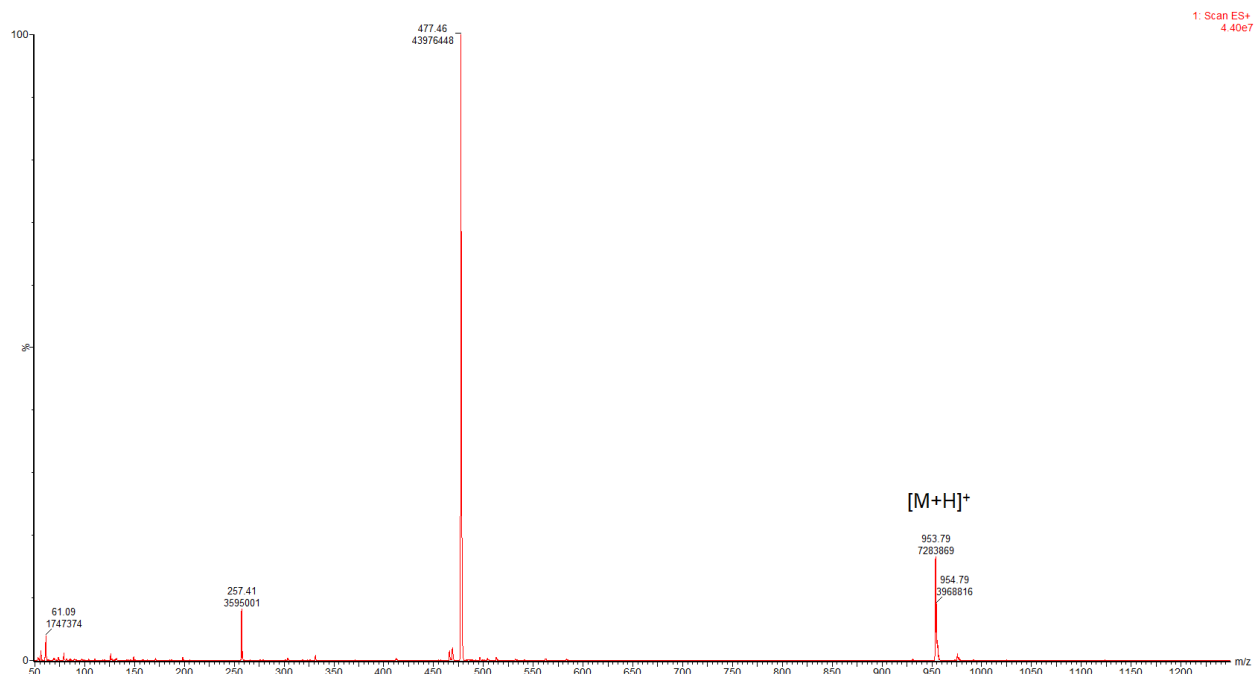


Figure S27. UPLC-MS profile of peptide 12.

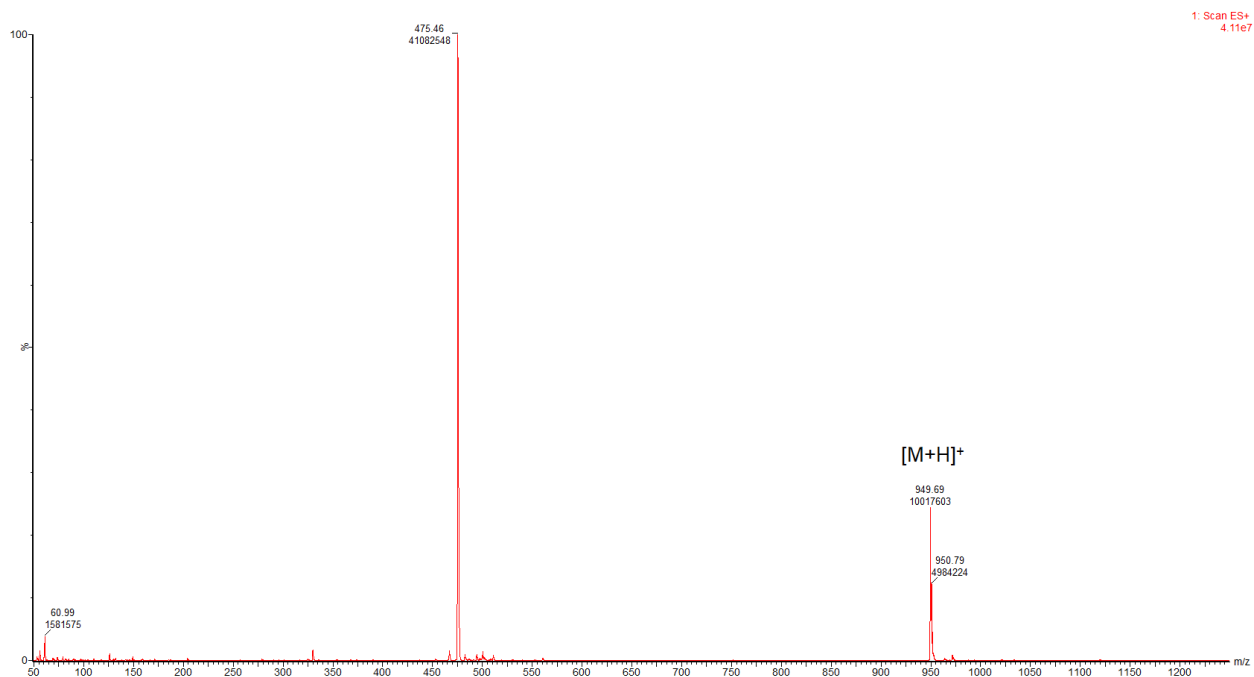
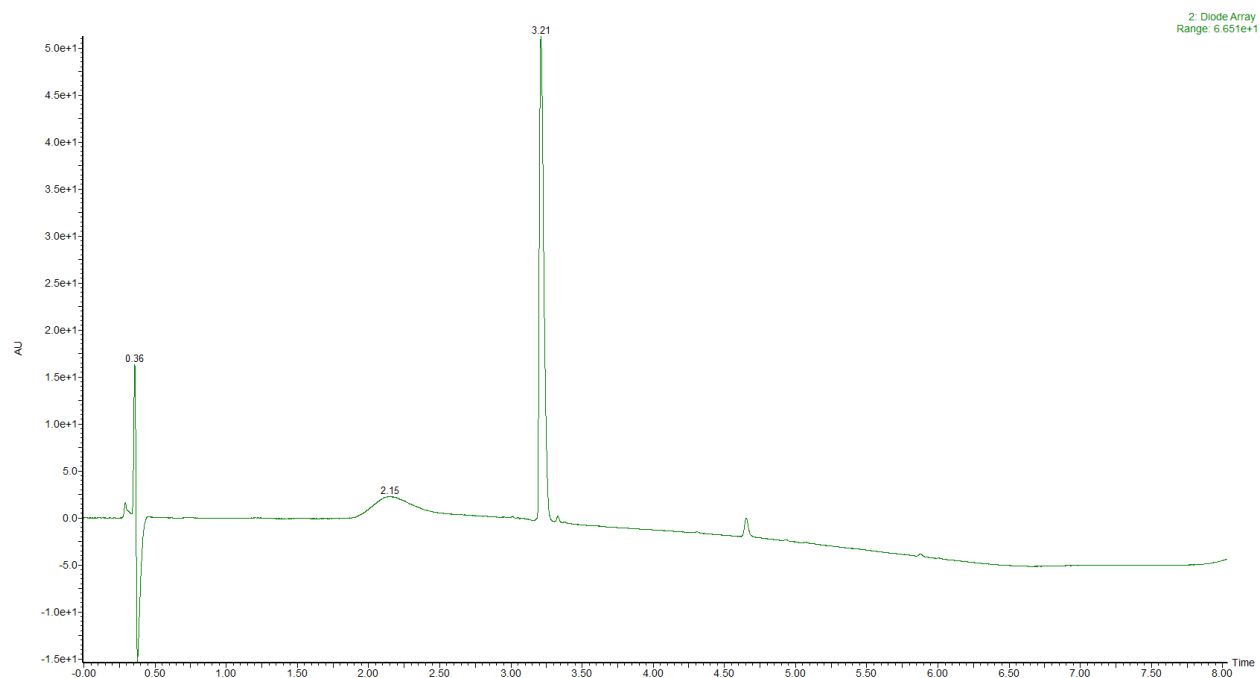
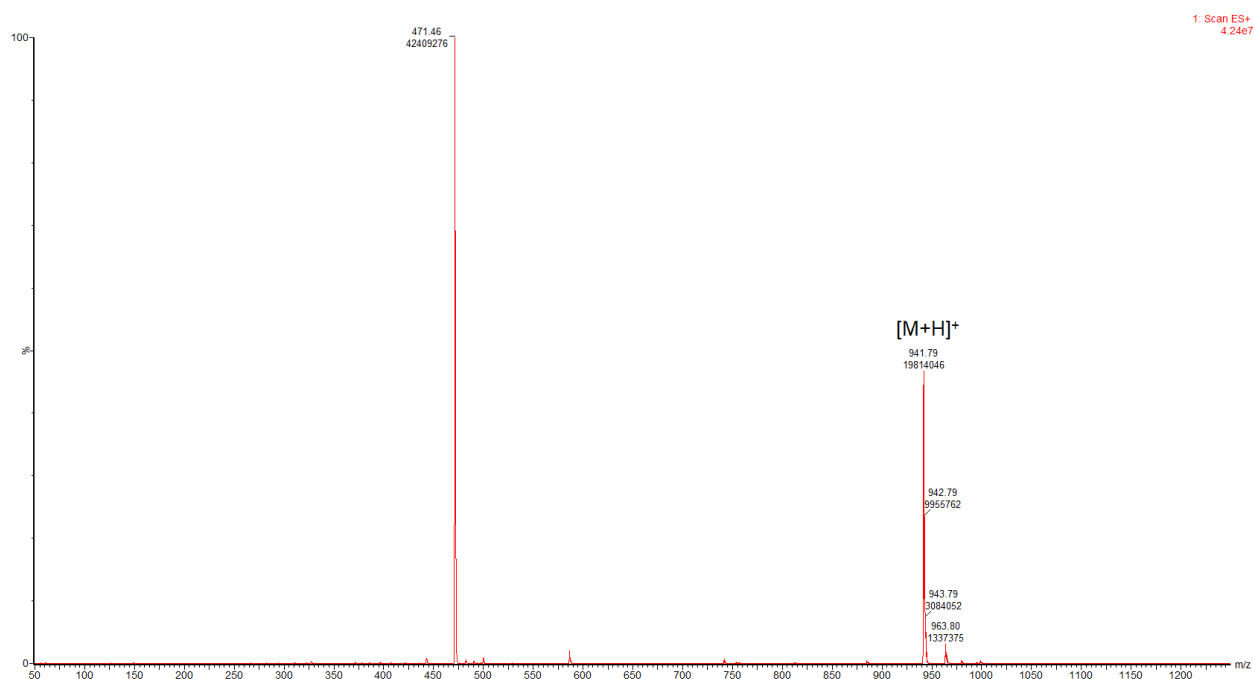
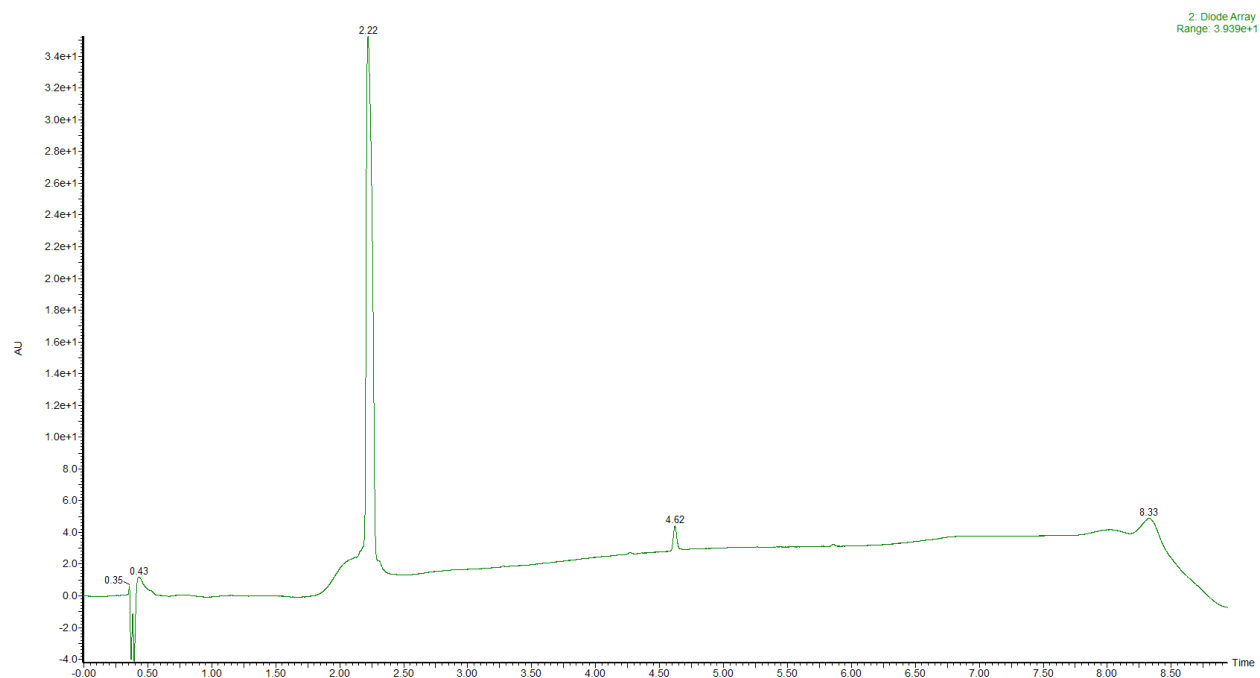


Figure S28. UPLC-MS profile of peptide **13**.



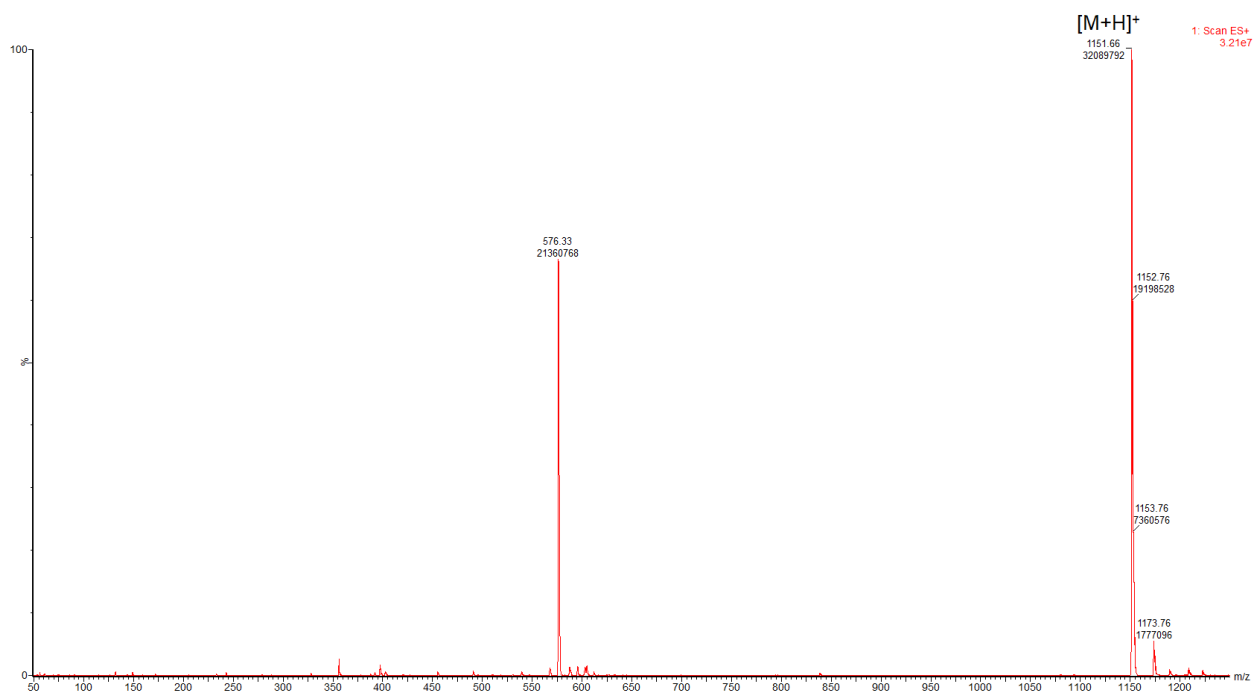
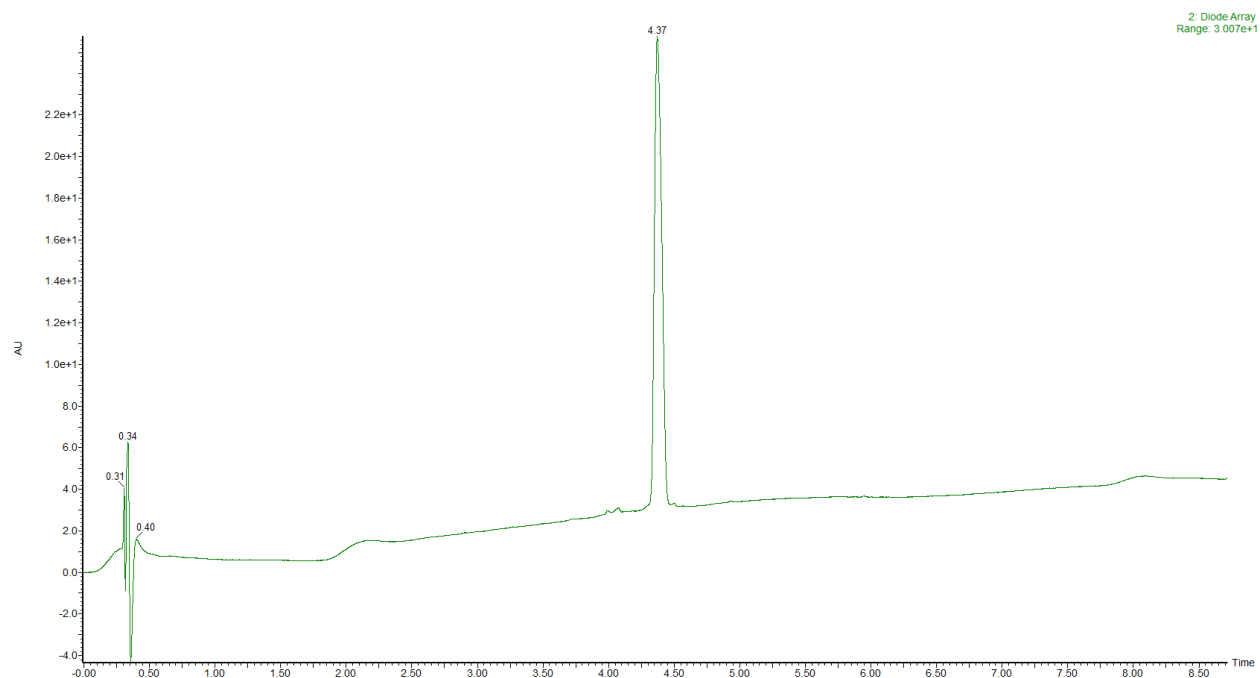


Figure S30. UPLC-MS profile of peptide **10**.

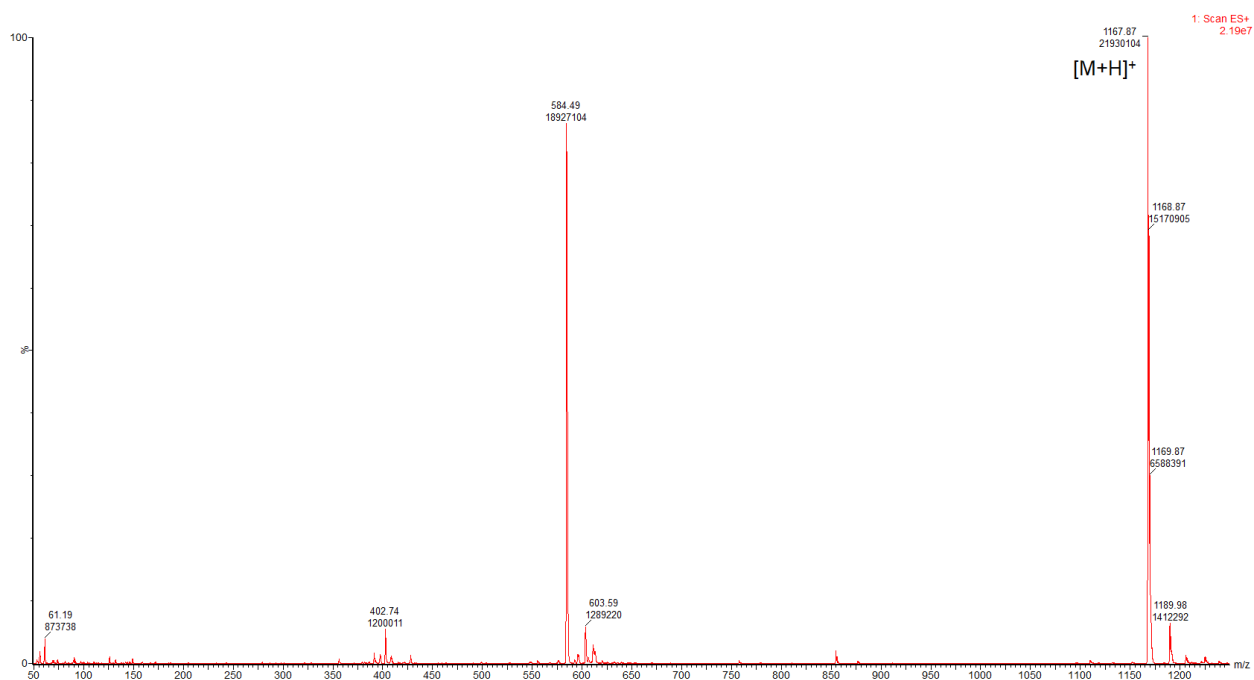
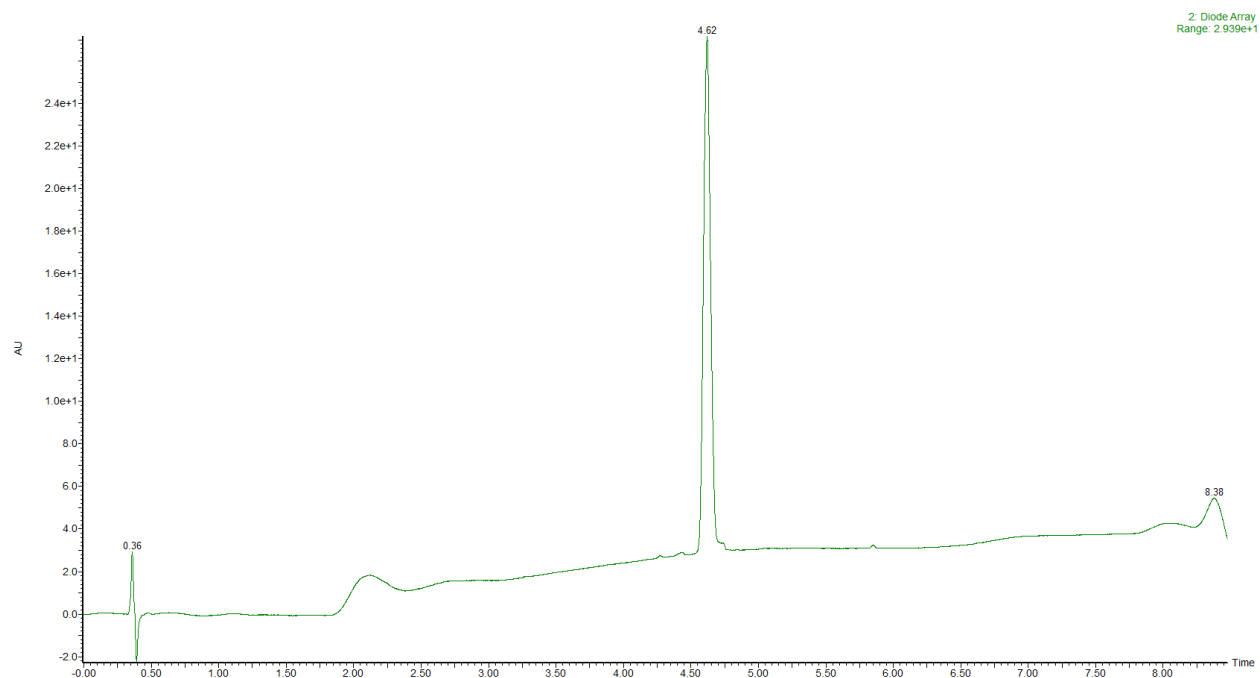


Figure S31. UPLC-MS profile of peptide 9.

Computational methods

Crystal structures of human and *Danio rerio* HDACs shown in Table S5 were downloaded from the Protein Data Bank PDB⁴. In case of mutated forms of HDAC isoforms (that are required to co-crystallize a substrate peptide) the mutations were modified into the wild type form. Protein preparation was done using MOE2018.01 protein preparation module⁵ by adding hydrogen atoms, assigning protonation states and minimizing the protein using the AMBER 14 EHT force field and the GB/SA solvation model. Substrate peptides **1** and **2** were prepared in MOE2018.01⁵ using the Protein builder module. To reduce the conformational freedom of the ligands we used only the central pentapeptide GGK_{ac/thioac}FF with acetylated N-terminus and amidated C-terminus. Molecular docking was performed using the program GOLD and Goldscore as scoring function⁶. Water molecules mediating hydrogen bonds between HDAC and ligand in the crystal structure were considered for the ligand docking. The zinc ion was used to define the center of the binding pocket for docking (radius 20 Å). Protein hydrogen bonds in GOLD were used to the backbone CO of the conserved Gly as well as to the side chain of the conserved Asp/Ser located at the rim of the HDAC binding pocket (both hydrogen bonds are observed in all crystal structures of peptides substrates). We used the water toggling mode in GOLD where the ligand is able to displace a water molecule. 100 docking poses were calculated for peptide **1** and **2** in each HDAC structure. The top-ranked docking poses were selected based on Goldscore.

References

- (1) Emiliani, S.; Fischle, W.; van Lint, C.; Al-Abed, Y.; Verdin, E. Characterization of a human RPD3 ortholog, HDAC3. *Proceedings of the National Academy of Sciences of the United States of America* **1998**, *95*, 2795–2800, DOI: 10.1073/pnas.95.6.2795.
- (2) Fischle, W.; Emiliani, S.; Hendzel, M. J.; Nagase, T.; Nomura, N.; Voelter, W.; Verdin, E. A new family of human histone deacetylases related to *Saccharomyces cerevisiae* HDA1p. *The Journal of biological chemistry* **1999**, *274*, 11713–11720, DOI: 10.1074/jbc.274.17.11713.
- (3) Kutil, Z.; Skultetyova, L.; Rauh, D.; Meleshin, M.; Snajdr, I.; Novakova, Z.; Mikesova, J.; Pavlicek, J.; Hadzima, M.; Baranova, P. *et al.* The unraveling of substrate specificity of histone deacetylase 6 domains using acetylome peptide microarrays and peptide libraries. *FASEB journal : official publication of the Federation of American Societies for Experimental Biology* **2019**, *33*, 4035–4045, DOI: 10.1096/fj.201801680R.
- (4) Berman, H. M.; Westbrook, J.; Feng, Z.; Gilliland, G.; Bhat, T. N.; Weissig, H.; Shindyalov, I. N.; Bourne, P. E. The Protein Data Bank. *Nucleic Acids Research* **2000**, *28*, 235–242.
- (5) Molecular Operating Environment (MOE), 2018.01; Chemical Computing Group Inc., 1010 Sherbooke St. West, Suite #910, Montreal, Qc, Canada, H3a 2r7, 2012
- (6) Improved Protein-Ligand Docking Using GOLD M. L. Verdonk, J. C. Cole, M. J. Hartshorn, C. W. Murray and R. D. Taylor, *Proteins*, *52*, 609-623, 2003